Drivers of roe deer use in fragmented forest landscapes; implications for management in the context of policy driven forest expansion

Saudamini Venkatesan[1], Benjamin M. Marshall[2], Mark S. Greener[2], Anna Kinghorn[2], Isla Sligo-Young[1], Richard Hassall[3], Robin Gill[4], Ben McKeown[5], Jeanette Hall[5], Roman Biek[2], Lucy Gilbert[2], Thomas A. Morrison[2], and Caroline Millins*[1]

[1]**Department of Livestock and One Health, Institute of Infection, Veterinary and Ecological Science, University of Liverpool, United Kingdom**
[2]**School of Biodiversity, One Health and Veterinary Medicine, University of Glasgow, UK**
[3]**UK Centre for Ecology and Hydrology, Wallingford, UK**
[4]**Forest Research, Alice Holt Lodge, Farnham, UK**
[5]**NatureScot, Torlundy, Fort William, UK**
*`Caroline.Millins@Liverpool.ac.uk`

Abstract

Forest expansion is a major current land use change across Europe. How this will affect the forest use of the most common European wild ungulate species, roe deer (*Capreolus capreolus*), and associated forest ecosystem services and disservices is poorly understood. Using a forest-agricultural mosaic landscape in northeast Scotland, we selected forests across a size and connectivity gradient as a proxy of expansion. We predicted that roe deer forest use estimated using camera traps would be driven by; i) higher structural and functional forest connectivity at a landscape scale, ii) within-forest structural characteristics including higher shrub density, deciduous cover and lower canopy cover, and iii) lower human usage. In line with predictions, roe deer preferred more connected forests and smaller forests in areas of the landscape with higher forest edge density. Within forests, roe deer preferred forest edge, and usage increased with higher tree density and variation in tree diameter, supportive of a preference for structurally complex forests. Human usage of forests was associated with lower roe deer use. This study has implications for current and future forest management. Firstly, targeted monitoring of forest patches predicted to have high roe deer usage for impacts could inform priorities and approaches to deer management. Secondly, as forest configuration changes with expansion policies, this study provides insights into how deer usage may change. We highlight how this knowledge can be used in forest planning to optimise deer management to minimise disservices to forestry, biodiversity and human and livestock health.

Keywords

Roe deer, habitat use, woodland, landscape, connectivity, functional connectivity, fragmentation

Graphical Abstract

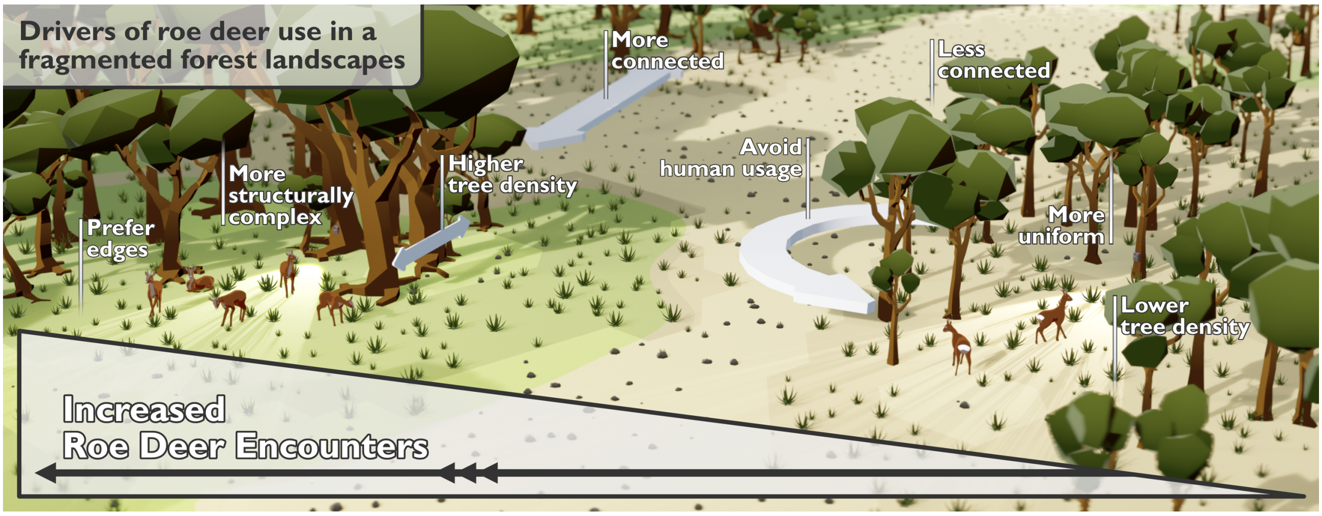

1 Introduction

Policy targets to expand forests across Europe to enhance biodiversity and mitigate climate change are driving large-scale changes to forest extent and connectivity. Between 1990 and 2023 forest cover in Europe expanded at a rate of 0.3% per year resulting in an increase of 19.3 million hectares of forest, and forecasts are for this trend to continue (Forestry Europe, 2020). In the United Kingdom and other parts of Europe, there is a policy focus on expanding native woodlands and reconnecting ecological networks to support biodiversity (DEFRA, 2018; Scottish Government, 2019, 2024). This major land use shift will significantly change the spatial distribution of resources across landscapes for wildlife species. How this will impact behaviour, movement and habitat selection of key forest ungulate species such as roe deer (*Capreolus capreolus*) is not well understood and is important for forest management and restoration.

Roe deer are non-specialist herbivores which thrive in disturbed heterogeneous forest landscapes such as those created during forest expansion (Gill et al., 1996; Hewison et al., 2001; Abbas et al., 2011). In this paper, the term forest is used for a wooded area at least 0.5ha with canopy cover >20%, and includes both native woodland and commercial forestry (Forestry Commission, 2019). As the most abundant and widespread wild herbivore in Europe, roe deer can act as ecosystem engineers due to their ability to impact ecological processes and nutrient cycling through grazing and browsing (Fuller & Gill, 2001; Côté et al., 2004). However, at high densities, roe deer can be responsible for a range of disservices to forestry, biodiversity and human and livestock health. Roe deer can be detrimental for forest restoration and regeneration by browsing on woody vegetation and forest specialist ground flora, adversely affecting biodiversity and timber production (Joys, Fuller & Dolman, 2004; Gill & Fuller, 2007) and can also impact surrounding agricultural resources (Putman & Moore, 1998). With respect to biodiversity, sustained heavy browsing is the most widespread threat to designated forest features in Scotland (NatureScot, 2016). Further, overgrazing is the second largest negative pressure on protected sites after invasive species (NatureScot, 2025). Where high deer and human activity co-occur, there can be risks to humans, by increasing the risk of traffic collisions (Nelli et al., 2018; Lush & Lush, 2026), increasing the risk of transmitting shared parasites and pathogens to livestock (Böhm et al., 2007) and increasing the risk of some zoonotic pathogens, particularly those transmitted by the tick *Ixodes ricinus* (Linard et al., 2007; Rizzoli et al., 2009; Gilbert et al., 2012; Mysterud et al., 2016). Thus, knowledge of how landscape and forest characteristics influence roe deer use of forests is important to understand for current and future forest management and for managing potential disease risks to livestock and people.

Roe deer habitat selection at the home range level is primarily driven by needs for shelter, feeding, and reproduction (Mysterud, Lian & Hjermann, 1999; Saïd & Servanty, 2005). In mixed, multi-use landscapes, ungulates typically utilise forests for cover and browsing, and may move into areas of neighbouring agricultural land where they provide high quality feeding resources (Bjorneraas et al., 2011). Therefore, landscape structure may influence large herbivore behaviour through a 'risk-resource' trade off (Martin et al., 2018) as they balance foraging and feeding with factors like predation, hunting pressure and other human disturbance (Brown, Laundré & Gurung, 1999). In Europe, roe deer thrive in fragmented forest-agricultural landscapes and show strong preferences for forest habitat and forest–agricultural ecotones (Hewison et al., 2001; Morellet et al., 2011; Lovari, Serrao & Mori, 2017; Marshall et al., 2026b) with predation, roads, urban areas and hunting acting as deterrents (Loro et al., 2016; Martin et al., 2018; Ciach & Fröhlich, 2019). Their use of open habitat is influenced by their perception of risk and affected by the time of day, season and distance from a forest, with strong preference to stay within or nearby forest (Martin et al., 2018; Torretta et al., 2025). Therefore, more structurally connected forest patches would be expected to have higher roe deer usage as compared to more isolated forests which could pose higher risks from traversing open habitats. This effect could be modulated by this species' preferences for forest edges and could result in an intermediate level of structural connectivity having highest usage. In contrast, the functional connectivity of a forest, as distinct from structural connectivity, also includes non-forest habitat (such as open grassland, moorland or roads) used by roe deer as they move between forests. Functional connectivity of forests, estimated from analysis of deer movement patterns, is therefore expected to explain roe deer habitat use more comprehensively than structural connectivity.

Forest characteristics which describe the quality of forests for shelter and feeding have also been found to influence usage by roe deer (Schwegmann et al., 2023). The influence of these forest characteristics is likely to be affected by the landscape context and availability of resources nearby; for example, relatively poor-quality forest for foraging may be used for shelter when there are high quality feeding resources in nearby agricultural fields. Roe deer have been found to prefer younger broadleaf forests (Torres et al., 2011; Spake et al., 2020; Marshall et al., 2026b) with higher quality and more palatable ground vegetation (Bobrowski, Gillich & Stolter, 2020). Higher forage availability associated with a more open canopy and higher light transmittance has been associated with higher roe deer use (Ramirez et al., 2023). Within-forest heterogeneity can increase opportunities for sheltering, and forests with higher shrub cover, tree species richness and variation in tree diameter at breast height have been found to have higher deer habitat use (Spake et al., 2020; Schwegmann et al., 2023). Deadwood left in forests to improve biodiversity and nutrient cycling can reduce roe deer habitat use, possibly by impedance of roe deer movement (Schwegmann et al., 2023). Forest usage by roe deer can also be driven by the intensity of human recreational use of forest patches, due to human disturbance and hunting pressure (Bonnot et al., 2013; Mols et al., 2022a,b). Within forests, lower roe deer usage has been found near more frequently used trails compared to less frequently used trails in recreational forest parks (Mols et al., 2022a,b).

Studies quantifying roe deer habitat use in the UK have largely used indirect measures such as dung and track counts (Putman et al., 2011; Gilbert et al., 2012). Relatively few studies have quantified roe deer habitat use in the UK directly using camera traps, but see (Hsing et al., 2022; Mason et al., 2022), and none designed at a landscape scale. Whereas dung counts record previous deer space use over an indeterminate period (from minutes to several weeks before survey); they only record where the deer dropped dung, not their entire space use; and the species of deer is not always identified. Additionally, indirect methods can have lower detectability rates compared to direct camera trapping methods and are sensitive to vegetation structure, climate and weather conditions (Pfeffer et al., 2018; Wearn & Glover-Kapfer, 2019; Dickinson, Millins & Biek, 2020). Other studies have used alternate proxies for relative density or population change, such as gaming kill counts or herbivory damage (Noble et al., 2012; Spake et al., 2020),. However, the latter indicator conflates the impacts resulting from deer presence with actual deer habitat use, relative abundance or density; thereby, making it difficult to disentangle the relationship between the two. In contrast, cameras record real-time space use for a known deer species over a known period and record their presence in that area.

In this study we measured roe deer habitat use in forests selected across a landscape gradient of forest patch size and connectivity, as a proxy of forest expansion using camera traps. The overarching aim of this study was to determine the wider landscape and between and within forest structural habitat drivers on roe deer forest usage. The study landscape was a mosaic of fragmented forest and agricultural land in Aberdeenshire, Scotland, an area currently undergoing forest expansion (Scottish Government, 2019). Camera traps were used to measure roe deer encounter rates as an estimate of the intensity of forest use by roe deer, and to measure human encounter rates as a measure of human recreational use of forest patches. We firstly predicted that roe deer forest use will be higher in more connected forests, as this will offer increased opportunities for shelter and minimise risks which are likely to be higher in open habitats. Further we predict that this relationship may be non-linear due this species preference for forest edge habitat (P1). We predicted that the effects of functional connectivity on roe deer forest use, which accounts for behaviour and relative preference or avoidance of intervening habitats such as open arable and pasture, roads and urban environments (Marshall et al., 2026b) would be greater than effects of forest connectivity measured as a structural metric which does not account for composition of the intervening matrix (Hanski, 1998) (P2). Thirdly, we predicted that roe deer forest use will be affected by the structural characteristics of the forest patch and that forests with a higher percentage of deciduous trees, higher shrub cover and lower canopy cover will have higher roe deer forest use due to increased attractiveness for feeding and shelter (P3). Fourthly, we predicted that roe deer forest use would be higher nearer the forest edge, reflecting this species preference for edge and ecotonal habitat (P4). And finally, we predicted that roe deer forest use would be modulated by human infrastructure and activities in the landscape measured as the proportion of urban landcover in the surrounding landscape (Martin et al., 2018) and encounter rates of humans on camera traps, as a proxy of disturbance (Brown, Laundré & Gurung, 1999) (P5).

2 Methods

2.1 Study landscape

The study was conducted in forests distributed across a 2,780 km^2 fragmented forest and agricultural landscape in Aberdeenshire, Scotland in 2022-2023 (57°8.75'N, 2°42.24'W, Fig. 1). The landscape is composed of a mosaic of different habitats: heather moorland and acid grasslands which cover 33.4% of the landscape, some of which are used for extensive livestock grazing; 14.5% arable land used for growing crops; 25% improved grassland, used for grazing or producing silage for livestock; and 25% of the land area is fragmented forest patches. With an average population density of 59 persons per km^2, built-up land covers only 1.7% of the area, mostly concentrated in farmhouses, small towns and villages. Land cover proportions are obtained from UKCEH Land Cover Maps 2023 (Morton et al., 2024). Ethical permission for the study was granted by the University of Liverpool Veterinary Research Ethics Committee, reference VREC1183.

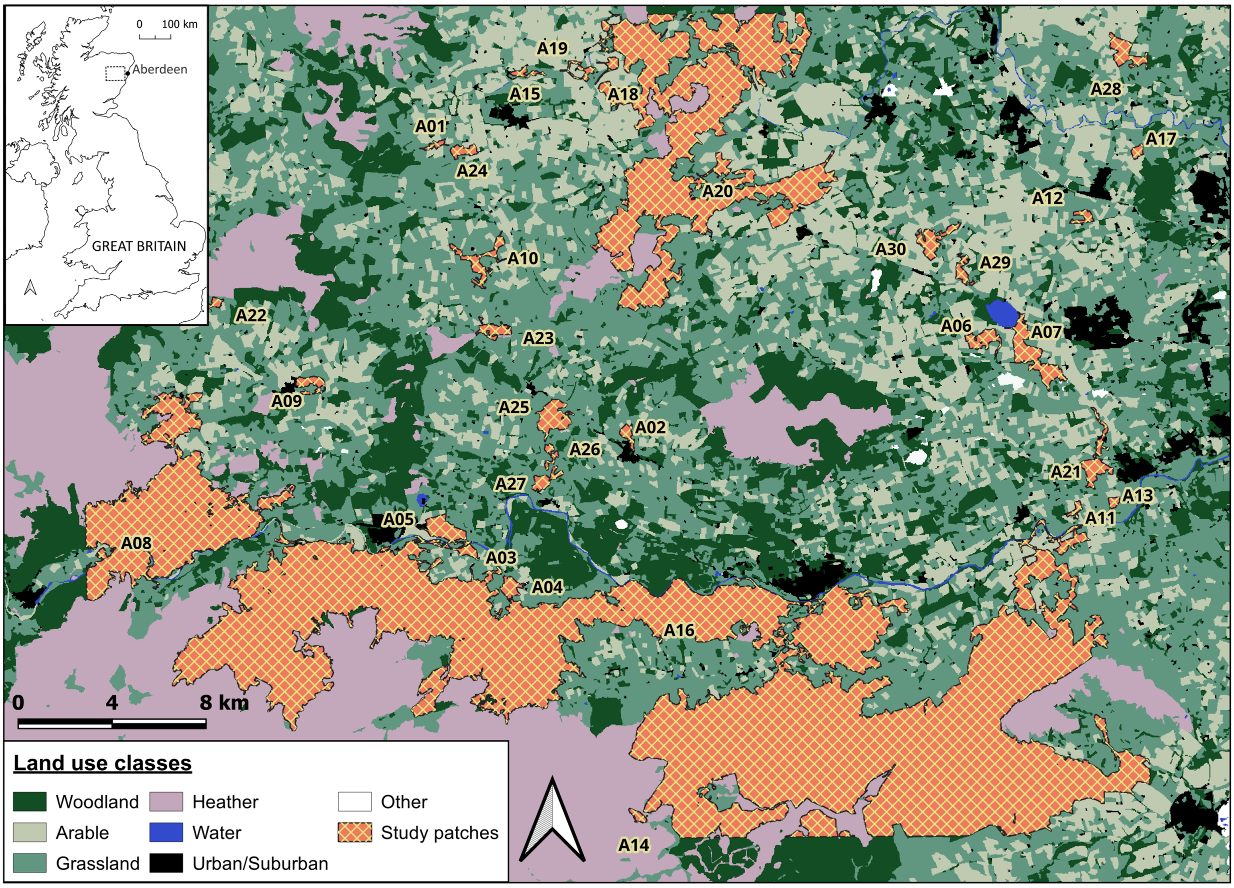

Figure 1. Map of the study landscape in Aberdeenshire, Scotland, UK with the study forests highlighted and labelled. Land cover use classes were derived using the UKCEH Land Cover Map 2023 (Morton et al., 2024).

2.2 Forest site selection and landscape metrics

We selected 30 forests along a gradient of forest patch size and connectivity. Forest polygons were identified from the UKCEH Land Cover Map 2021 (Marston et al., 2022) and 30 forests were sampled equally across five quantiles of forest area and two quantiles of forest structural connectivity (Fig. 1, Fig A1.1). Forests smaller than the minimum estimated home range of a roe deer (0.16 km^2) were excluded as candidate forests to ensure the study forest patches were large enough for resident roe deer populations. The mean patch size and connectivity index of the 30 study forests were 12.45 km^2 (Range: 0.17 – 224 km^2) and 17.09 (Range: 0.22 – 119), respectively (Fig A1.1). All forests selected had no deer fencing.

Forest structural connectivity was estimated using a distance weighted area metric, by taking a sum of the area of forests >0.5ha within a buffer of 750 m from the focal forest edge, weighting the areas by the distance between the surrounding forest patch and the focal forest patch [Further details in Appendix, sections A1.1 & A1.2); Bender, Tischendorf & Fahrig (2003); Hanski (1998)]. For inclusion in the structural connectivity metric, a threshold of forest patch size of greater than 0.5ha was used in accordance with UK National Forest Inventory definition of forests (Forestry Commission, 2019). The buffer size of 750m was selected as being biologically relevant as it corresponded to an estimation of roe deer home range in Aberdeenshire (Marshall et al., 2026b).

The proportions of arable, grassland, forest, urban land cover and forest edge density within a 750 m buffer from the edge of each forest patch were obtained for each of the study forests by combining the finer land use classifications in the UKCEH Land Cover Map (Morton et al., 2024) into broader classes (Further details in Appendix, Section A1.2; Table A1.1). The grassland category in this study combines the finer land-use classifications of improved, neutral, calcareous and acid grassland, and heather and heather grassland. Heather and heather grassland were included in the grassland category, as this landcover type was absent in the surrounding buffer of most forest patches (n=25/30). The largest nine of the thirty forests (> 80 ha) were surveyed with camera traps within a smaller focal area to provide comparable sampling effort per unit area to smaller forests and to ensure that distance between cameras within a patch did not increase with increasing patch size. For these forests, landscape metrics were extracted corresponding to a 750m buffer around the edge of this focal sampled area. The focal area was defined by drawing a circle centred on the centroid of all camera trap deployments using a radius equal to the distance from the centroid to the camera farthest away.

2.3 Functional connectivity

Landscape-wide estimates of functional connectivity for roe deer were estimated by building on a habitat use model from GPS collared roe deer captured in the study landscape (Marshall et al., 2026b). The habitat use model aimed to determine roe deer preference for various land use types, as well as how their movements are altered within them (Marshall et al., 2026b). Coefficients of a population level Poisson habitat preference model were used as a basis to estimate landscape level movement resistance/conductivity for roe deer. We projected these coefficients of preference and movement ease via the UKCEH Land Cover Map landscape raster (Morton et al., 2024), using Ordnance Survey (2024) and Scholefield et al. (2016) to map the resistance impacts of roads and hedgerows respectively. This resulted in a landscape raster (at 25m resolution) mapping out the relative resistance movement resistance/conductivity for roe deer (See Appendix A1.3; Fig. A1.2). We converted the resistance mapping to functional connectivity using a random shortest paths approach (Panzacchi et al., 2016). This approach consisted of generating repeated random walk between forest patches (6 per pair of patches; 3,415 total patches), where the path routes where weighted by the estimated landscape resistance –areas of high resistance (as estimated from the Poisson habitat preference model) were less likely to house paths (see Appendix A1.3). We also ensured that the diffusion of the random paths matched the movement patterns of the roe deer (see Appendix A1.3; Fig. A1.3). Each random walk between patches produced a raster describing the likelihood of a roe deer crossing a cell (cell size was set to 25m matching the land cover data and resistance map resolution). When compiled together the resulting rasters to give a landscape level mapping of relative likelihood of a roe deer using that area to move between patches. We standardised this final landscape layer to be between 0 and 1 (where 0 is low functional connectivity and 1 is high functional connectivity). For inclusion in statistical models, we calculated a mean connectivity score for each forest patch. This mean included all raster cells that fell within a forest patch. Although we had no spatial covariates to differentiate within forest movement resistance (beyond the low resistance of forest compared to non-forest land uses), the inclusion of within-patch connectivity values was important as patches between other patch pairing could serve as stepping-stones. Further details can be found in the Appendix (section A1.3) concerning the estimation of path diffusion, required computation optimisations, and the validation measures using the roe deer movement data.

2.4 Forest structural habitat characteristics

Forest habitat surveys were carried out in July-September 2023 at each of the forest sites, to collect data on forest structural habitat characteristics specifically, shrub, sapling and tree density, variation in tree diameter at breast height (DBH), tree species richness, tree canopy closure and woody debris based on previously described methods (Fuentes-Montemayor et al., 2020). In each forest patch, surveys were carried out along five randomly generated 100 m transects located in the area where camera trapping was conducted. Every transect had 10 sampling points resulting in 50 sampling points per forest patch.

At each sampling point along a transect, 4 quadrants were identified by laying two sticks crossing one another in the north-south and east-west directions respectively. The four nearest trees (defined as woody plants greater than 2m in height, and diameter at breast height > 5cm), one in each quadrant were located, and the diameter at breast height (DBH, cm), tree species and distance from the sampling point were recorded. Tree density (tree per m^2) was then calculated at every sampling point using the point-quadrant method (Hill, 2005) using the equation

1/(Mean sampling point-to-tree distance)^2. At each sampling point, woody debris was scored from a scale of 1-3 with the indices corresponding to the following: 1 – leaf litter and twigs $<=$ 1 cm in diameter, 2 – larger branches $<=$ 10 cm, 3 – coarse debris $>$ 10cm in diameter. Tree canopy closure (%) was estimated using an Android app (CanopyViewer, `https://apkpure.com/canopy-surveyor/skipper.com.canopyviewer`). Shrub and sapling density was estimated at 3 sampling points (1st, 5th, 10th) per transect by counting the number of shrubs (woody bushes with height between 40 cm and 2 m) and saplings (plants with DBH $<=$ 5cm and height $>$ 2m) within a circle of radius 15m centred at the sampling point.

For inclusion in statistical models, forest patch-scale tree, shrub and sapling densities and tree canopy closure were estimated by averaging across all sampling points within a site. Variation in tree DBH was obtained by taking the standard deviation of tree DBH across all sampling points. Tree species richness was estimated by counting the number of distinct tree species across all sampling points within a forest. For woody debris, the most frequent value (mode) was taken as a forest patch scale index of deadwood.

We also obtained forest patch deciduous cover and distance of the camera location to the edge of the forest patch using the UKCEH Land Cover Map (Morton et al., 2024). The proportion of deciduous cover within each forest patch was obtained by the proportion of 25 x 25m cells within a forest polygon categorised as 'Deciduous woodland' in the Land Cover Map. To test if roe deer preferred forest edges compared to forest interior, the distance of each trail camera position to the edge of forest was obtained by estimating the Euclidean distance between the camera location coordinates and the closest edge of the forest.

2.5 Use of forests by roe deer and humans

To estimate roe deer encounter rates as a measure of forest habitat use, we carried out camera trap surveys conducted from May to November 2022 and April to September 2023 in the selected forests in Aberdeenshire (Fig. 1). Surveys were carried out in the spring and summer months only as they were conducted as a part of a larger project quantifying the availability of forest vertebrates to the seasonally active tick vector *Ixodes ricinus* (results reported in Venkatesan et al., in prep). In each forest, three trail cameras (Spec Ops Elite HP5, Browning, Morgan, UT, USA) were deployed at randomly generated locations within the forest patch and moved every 3-5 weeks, giving a total of 27 sampling points per forest. Deployment locations were generated randomly ensuring that locations were at least 30 m apart and at least 20 m away from forest edge. Methods were based on those previously described (Hofmeester, Marcus Rowcliffe & Jansen, 2017). Briefly, cameras were mounted on a tree nearest to the random survey point, and positioned at a height of 40 cm with a field-of-view parallel to the ground, facing north or southwards to avoid direct sunlight during dawn and dusk (Hofmeester, Marcus Rowcliffe & Jansen, 2017). Cameras were positioned to avoid trails or paths to minimise sampling bias in estimates of wildlife usage, and for privacy reasons. Additionally, as mentioned in Section 2.2, cameras were deployed within a smaller sub-region in the 9 largest patches ($>$80 ha) to ensure that mean and median distance between cameras was not associated with patch size (further details in Section A1.4). Cameras were programmed to capture still images using motion detection, with a 1-second delay between images, and vegetation was pruned within 3m of the camera to reduce false triggers and obstruction to field of view.

We used the software Wildlife Insights (www.wildlifeinsights.org) (Ahumada et al., 2020) to identify roe deer and humans detected in camera trap images using a combination of AI automated and manual classification. Deployments shorter than 7 days due to camera malfunction were removed from the analysis (33/723 deployments). First, we evaluated the performance of the Wildlife Insights in-built algorithm in identifying false triggers (with no animal present in the frame) and deer species, within a sub-sample of manually identified images. The algorithm identified false triggers with a precision of 99% and deer with a precision and recall of 97.7% and 89.4% respectively (further details in Appendix A1.5). Therefore, we used the algorithm to remove blank images and to classify the deer images. All images classified as "non-deer" were reviewed manually to classify any overlooked deer images as well as human images. Once classified as roe deer or human, images were grouped into sequences, defined as consecutive images taken within a 15-minute period. For each sequence, the maximum number of animals (roe deer or humans) per image was calculated. The number of sequences and maximum animal count were multiplied and divided by the deployment duration (in days) of that camera to estimate the encounter rate defined as the number of observations per day at each deployment. A 15-minute threshold was chosen to reduce overdispersion from overcounting the same individuals while still reflecting the intensity of use at each deployment location (Hofmeester, Marcus Rowcliffe & Jansen, 2017). Roe deer and human encounter rates were thus obtained at each deployment location per focal forest. Since cameras were placed to avoid trails or paths to reduce bias in recording wildlife species, this may underestimate human encounter rates at the deployment-scale. We therefore obtained a relative measure of human recreational use at the forest-scale by averaging deployment-level human encounter rates across all deployments within each focal forest for use in the statistical analyses.

2.6 Statistical analysis

All statistical analyses were carried out using R (v.4.4.1) (R. Core Team, 2024) and RStudio (v.2024.09.1+394) (Posit team, 2024). Generalised Linear Mixed Models (GLMMs) were fitted using the package glmmTMB (v.1.1.10) (Brooks et al., 2017). Models were assessed for collinearity between explanatory variables by calculating Variance Inflation Factors (Zuur, Ieno & Elphick, 2010) using the package performance (v.0.13.0) (Lüdecke et al., 2021). Other model diagnostics e.g., testing for normality, overdispersion, zero-inflation and outliers were carried out using the package DHARMa (v.0.4.7) (Hartig, 2022). Stepwise backward model selection was carried out on the full models using the drop1 function in R to obtain the final models with the lowest AIC (Bolker et al., 2009). All numeric explanatory variables were mean-centred and scaled.

2.6.1 Variable Selection

To avoid inclusion of colinear landscape variables and overfitting the statistical models, relationships between variables were first explored using pairwise correlation tests (Fig. A1.1). Where landscape and forest variable pairs with $r > 0.7$ were identified, the variables which were most closely related to the study questions were retained to be included in the full model. The proportion of forest in a 750m buffer surrounding the focal forest was dropped as it was significantly correlated with both edge density ($r = 0.71$, $p = <0.001$) and log-transformed forest patch area ($r = 0.84$, $p < 0.001$). Additionally, edge density and the proportion of grassland in a buffer surrounding the forest were also excluded from the full model as they had Variance Inflation Factor >4.

2.6.2 Model fitting

To assess how landscape metrics and within-forest characteristics influence habitat use by roe deer and test predictions P1 and P3-5, we fitted a Generalised Linear Mixed Model (GLMM) with the total number of roe deer observations at each deployment as the response variable with a negative binomial error distribution and log-transformed deployment survey duration (days) as an offset (Model 1). Fixed explanatory variables in the full model included log-transformed forest area (patch size), log-transformed forest structural connectivity, the proportion of arable, and proportion of urban land cover within a 750m buffer surrounding each forest, the proportion of deciduous cover within the forest, mean human encounter rate and forest habitat variables (listed in Tab. 1). We also included second-order effect of structural connectivity to test if forest patches of intermediate connectivity had the highest deer usage. Forest ID, year, and month were included as nested random effects to account for temporal variation in roe deer observations and repeated sampling within forest patches.

Since patch area was colinear with edge density and forest cover in a 750m buffer, and we expected that these variables would be important drivers of roe deer forest use, we conducted additional analyses replacing forest patch area with edge density and forest cover in a 750m buffer, keeping the other variables same as in Model 1.

Next, to test our prediction (P2) that roe deer functional forest connectivity would provide greater explanatory power of habitat use by roe deer, we fitted a second GLMM with the same response and random and fixed explanatory variables as above, substituting functional connectivity for structural connectivity and carrying out stepwise model reduction (Model 2).

Finally, to explore which landscape metrics predicted roe deer functional connectivity, we fitted a linear model with mean forest functional connectivity as a response variable. Explanatory variables included structural connectivity, urban and arable landcover and the % deciduous cover in the patch.

Table 1. Descriptions of fixed and random explanatory variables included in the full statistical models, with the number of roe deer observations per camera deployment as the response variable with negative binomial error and deployment duration (in days) as the offset. All explanatory variables were estimated at the forest scale, apart from deployment distance to forest edge. Two different models were fitted: one with structural connectivity and the other with functional connectivity; they otherwise had the same explanatory variables. Random effects were nested. All fixed variables were mean centred and scaled. The mean and range are provided for the raw variables prior to any transformations. Further details on the extraction of a) landscape variables and b) forest variables can be found in sections A1.1 and A1.2 and Methods, section 2.4 respectively.

Variable	Description	Spatial scale for analysis	Mean (Range)
a) Landscape variables			
Structural Connectivity (log)	Hanski connectivity metric quantifying proximity and size of surrounding forests within 750 m buffer	750m forest buffer	17.09 (0.22 - 118.79)
Functional connectivity	Mean forest patch connectivity derived from standardised likelihood of weighted random shortest paths.	Forest	0.06 (0.02 - 0.12)
Urban land cover	Proportion of urban land cover surrounding patch within a buffer of 750m	750m forest buffer	0.02 (0 - 0.14)
Arable land cover	Proportion of arable land cover surrounding patch within a buffer of 750m	750m forest buffer	0.25 (0 - 0.88)
Distance to forest edge	Distance (m) of deployed camera from forest patch edge	Camera deployment	77.3 (0.3 - 345.7)
b) Forest variables			
Area (log)	Forest patch area (sq. km); log-transformed	Forest	12.45 (0.17 – 228.14)
Shrub density (log)	Number of shrubs within 15m of sampling point, averaged across all sampling points within forest patch and log-transformed	Forest	6.9 (0 – 55.4)
Sapling density (log)	Number of saplings within 15m of sampling point, averaged across all sampling points within forest patch and log-transformed	Forest	55.524 (0-249.6)
Tree density	No. of trees / sq. m	Forest	0.09 (0.03 - 0.27)
Tree species richness	Number of unique tree species across all transects in a forest patch	Forest	4.931 (2 - 14)
Woody debris	Index scoring woody debris on forest floor (1-3); the mode across all sampling points was used per forest; categorical (2 levels)	Forest	2, 3 (categorical index)
DBH (SD)	Standard deviation of tree trunk diameter at breast height (cm) across all sampling points within a forest patch	Forest	12.9 (10.2 – 46)
Canopy closure (%)	Percentage closure of tree canopy, averaged across all sampling points within the forest patch	Forest	58.75 (39.66 – 76.06)
Deciduous cover	Proportion deciduous cover within the forest patch	Forest	0.35 (0 - 1)
Human encounter rate	Number of human observations per day, averaged across all camera deployments within the forest patch	Forest	0.06 (0 – 0.29)
c) Random effects			
Patch ID	Focal Forest identification (29 levels)		
Year	Year of sampling (2021, 2022)		
Month	Month of sampling (April-Oct)		

3 Results

Roe deer encounter rates were obtained from a total of 690 trail camera deployments placed between May and September/October in 2022 and 2023 from 29 forest patches, with an average of $\sim$24 (range: 20-27) deployment locations and 681 (range: 544 - 786) survey days per forest patch. Data from one forest was excluded due to large scale felling of trees in the second year of the study. The mean survey time for a camera deployment was roughly 29 days (SD: 8.6; range: 8 - 59). The mean roe deer encounter rate at the forest patch scale was 0.68 (SD: 0.29, range 0.15 - 1.24) roe deer encounters per day. At the deployment scale, roe deer encounter rates varied within forest patches (Fig: A2), with a mean of 0.55 (SD: 0.65, Range: 0 - 5.05) roe deer encounters per day. Among a sub-sample of 13,699 images which were manually screened (Appendix A1.5), we found only 3 occurrences of red deer (*Cervus elaphus*) limited to 2 out of the 30 forest patches in Aberdeenshire. All AI-classified images of deer from these two forest patches were manually screened and did not contain any red deer. In addition, all images classified as "non-deer" were manually screened in all forest patches to detect ungulates. Domestic cattle were detected at a single camera location each in two out of the 30 forests and no further red deer were detected.

3.1 Landscape scale drivers of roe deer forest usage

We obtained reduced models with structural connectivity (Model 1) and functional connectivity (Model 2) each having a positive effect on roe deer forest use (Fig. 2, Table A2.1). Both models accounted for roughly 27% of variation in roe deer forest use (conditional R^2: 0.272 & 0.273) with the fixed effect components of the model accounting for roughly 10% variation in roe deer forest use (marginal R^2: 0.097 & 0.095). Structural and functional connectivity were supported in the best fit model as linear effects on deer forest usage as models with second-order coefficients of connectivity had higher AIC and were removed during model selection (Table A2.5). Forests with higher structural connectivity to other forests had higher roe deer encounter rates (Model 1, RR: 1.18, 95% CI: 1.03 – 1.36) as did forests with greater functional connectivity (Model 2, RR: 1.24, 95% CI: 1.08 – 1.42), consistent with prediction P2. Forest patch area was a significant predictor in Model 1, with smaller forests having higher roe deer encounter rates (Model 1: RR: 0.82, 95% CI: 0.71 – 0.94); however, patch size was not retained post model-reduction in Model 2 (with functional connectivity) (Table A2.5).

As forest patch size was correlated with edge density and the proportion of forest landcover in a 750m buffer, separate analyses were carried out replacing forest patch size with each of these two variables. Forest edge density within a 750m buffer was positively associated with roe deer forest use (Table A2.2, RR: 1.21, 95% CI: 1.04 – 1.42) and the proportion of forest landcover was negatively associated with roe deer forest use (Table A2.3, RR: 0.78, 95% CI: 0.67 – 0.92). Urban and arable land cover in a 750m buffer around each forest were not retained in any of the final models (Table A2.5).

3.2 Forest structural habitat drivers of roe deer forest use

Consistent with prediction P4, distance of the camera location from forest edge had a small but significant effect, with deployments closer to the forest edge having higher deer encounters compared to those farther from the forest edge (Model 1, RR: 0.91, 95% CI: 0.83 – 0.99; Model 2, RR: 0.90, 95% CI: 0.83 – 0.98). In both Models 1 & 2, variation in tree DBH (Model 1, RR: 1.25, 95% CI: 1.08 – 1.44; Model 2, RR: 1.28, 95% CI: 1.11 – 1.48) and tree density (Model 1, RR: 1.22; 95% CI: 1.06 – 1.39; Model 2, RR: 1.22, 95% CI: 1.07 – 1.40) had a positive effect on roe deer forest use (Fig. 2, Table A2.1), consistent with prediction P3, while the mean human encounter rate in a forest patch had a negative effect on roe deer habitat use consistent with prediction P5 (Model 1, RR: 0.86, 95% CI: 0.74 – 0.99; Model 2, RR: 0.85, 95% CI: 0.74 – 0.99). In contrast to prediction P3, woody debris, percentage canopy cover, proportion deciduous cover, tree species richness, shrub and sapling density were not retained in the final models (Table A2.5).

3.3 Predictors of roe deer functional connectivity

The model explained $\sim$35% variation in roe deer functional connectivity (Table A2.4) with forest patch size and proportion of deciduous cover predicting functional connectivity but only with marginal significance. Contrary to expectations, structural connectivity was not a significant predictor of roe deer functional connectivity (Slope: -0.004, 95% CI: -0.011 – 0.002). Smaller forests had higher functional connectivity (Slope: -0.009, 95% CI: -0.015 – -0.002) as did more deciduous forests (Slope: 0.009, 95% CI: 0.000 – 0.018).

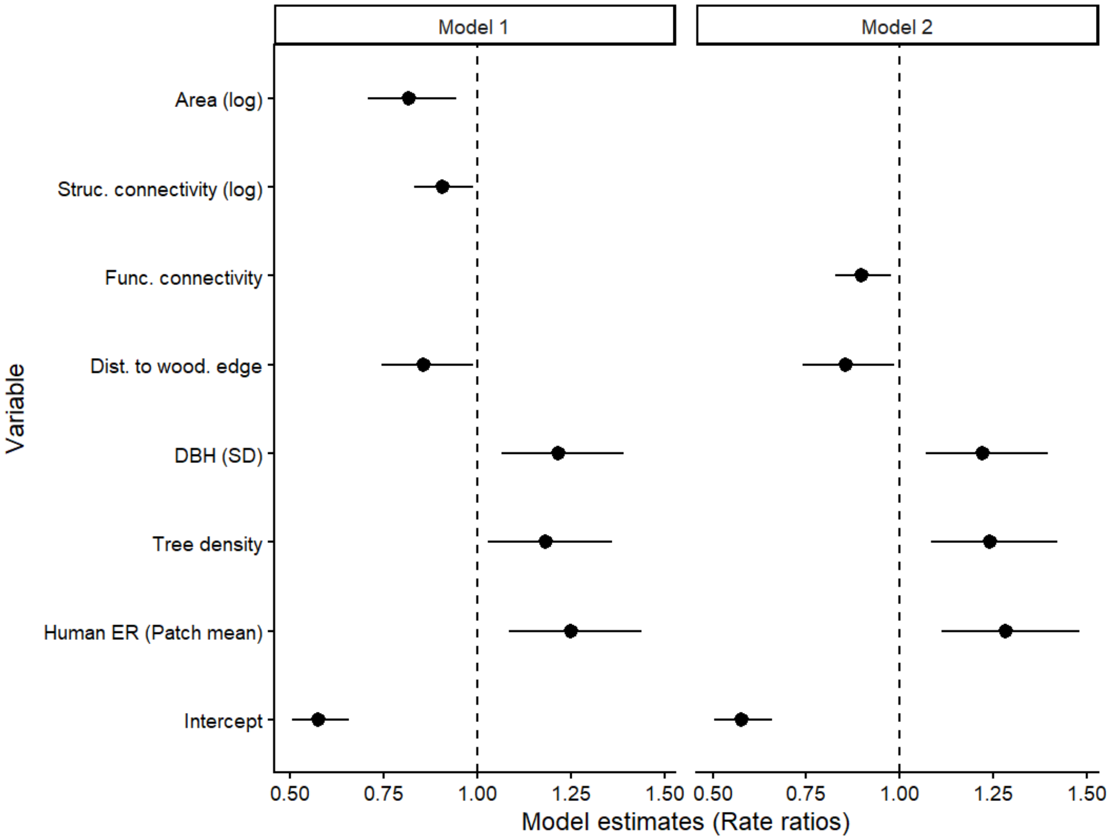

Figure 2. Output estimates of model coefficients affecting roe deer deployment level encounter rates from the final models obtained after step-wise model reduction. Model 1 included structural connectivity as an explanatory variable while Model 2 included functional connectivity, while all other explanatory variables were the same in the two full models. Points and error bars correspond to exponentiated model coefficients (rate ratios) of the final reduced negative binomial GLMMs and 95% confidence intervals respectively. Variables with coefficients greater than one (to the right of the dashed line) were positively associated with roe deer encounter rates while those with value less than were negatively associated with roe deer encounter rates. Human ER is the mean forest encounter rate of humans on camera traps; DBH (SD) is the standard deviation of the diameter of tree trunk at breast height. Final model summaries can be found in table A2.1.

4 Discussion

Using camera traps deployed across a gradient of forest patch size and connectivity, we found that roe deer living in a rural fragmented landscape preferred smaller, more connected forests. Within forests, roe deer showed a preference for utilising areas closer to the forest edge, and for forests with higher tree density and greater variability in tree size. Roe deer also exhibited lower use of forests that had higher human use.

4.1 Landscape drivers of roe deer forest patch use

Supporting our first prediction, we found that landscape features were strong determinants of roe deer habitat use. Consistent with prediction P1, forests which were more connected with other forests had higher roe deer usage. Results from previous studies on effects of connectivity on roe deer forest use are mixed, with some studies demonstrating a positive effect (Martin et al., 2018) while other studies do not find an effect (e.g., Schwegmann et al., 2023). In cases where studies do not detect an effect, this was suggested to be due to high levels of anthropogenic disturbance. Supporting this theory are studies demonstrating that functional connectivity can shift temporally depending on hunting pressure and other types of disturbance (Bonnot et al., 2013; Martin et al., 2018). Contrary to our expectations, functional connectivity [which we derived from GPS collar data from roe deer in the same study landscape; Marshall et al. (2026b)] did not have more explanatory power than structural connectivity: both types of connectivity explained equal amounts of variation in roe deer forest use (Section 3.4, Table A2.1). However, of particular interest, functional connectivity was not closely correlated with structural connectivity ($r = -0.125$, $df = 27$, $p = 0.52$), suggesting that the two connectivity metrics might be capturing different characteristics of the landscape. Forests with higher functional connectivity were characterised by smaller patch size and a higher proportion of deciduous cover partially reflecting our finding of a preference of roe deer towards smaller forests and consistent with previous studies that have found a preference for more deciduous forests (Spake et al., 2020; Zorzi et al., 2022; Ramirez et al., 2023; Schwegmann et al., 2023). The finding that structural connectivity performed as well as functional connectivity in predicting roe deer forest use suggests that the simpler structural connectivity metric could be used by forest managers to understand which forests are likely to be used more by roe deer and which may therefore have higher disservices. However, results also support that these connectivity metrics are giving different information about the landscape effects on roe deer forest patch usage, with functional connectivity providing added mechanistic insight.

We also found an effect of forest patch size on roe deer use, with preference for smaller forests. Forest patch size in many fragmented landscapes is often correlated with the proportion of forest and arable land in the surrounding matrix. This is the case in our landscape where forest patch size is highly positively correlated with forest cover in the surrounding landscape and negatively correlated with arable landcover (Fig. A1.6). In this type of landscape, deer could be utilising smaller forests for cover and protection and feeding in surrounding arable and ecotonal habitats. For example, in a mixed agricultural-forest landscape roe deer females showed higher use of crop fields that were near forests and hedgerows (Mysterud, 1996; Rigoudy et al., 2024). The higher use of smaller forests in our study could also be driven by a higher density of forest-edge ecotones. In our landscape, forest patch size was significantly negatively correlated with edge density, and replacing patch size with edge density in the model resulted in a significant positive effect of edge density on roe deer habitat use (see Appendix, Table A2.2). Roe deer have been shown to have a strong preference for forest edge habitats, due to field-forest ecotones providing a wide range of food resources from both forest and arable habitat, as well as providing cover from climatic factors and predation (Hewison et al., 2001; Torres et al., 2011; Feng et al., 2021). This is further supported by our finding that camera deployment locations closer to the forest edge had higher roe deer encounters compared to those located further inside the forest, consistent with our prediction P4.

4.2 Forest characteristics and roe deer forest use

Supporting our second prediction P2, we identified several structural forest habitat characteristics that were drivers of roe deer forest use. Forests with higher tree density, and higher variability in tree diameter had higher roe deer use. Variability in tree diameter can be interpreted as a measure of structural complexity of forests with older and more established natural and semi-natural forests containing trees of multiple species and ages which have more variation in tree diameter (Fuentes-Montemayor et al., 2020). Our results are consistent with a previous UK-wide study which found that the probability of damage by roe deer in forests increases with increasing tree density and age of the forest (Spake et al., 2020). Tree density is also positively correlated with canopy cover within our study landscapes, implying that roe deer may be preferentially selecting forests with more canopy cover. This contrasts with previous studies that have largely focused on extensive forest areas (Schwegmann et al., 2023) which found roe deer habitat use to be negatively associated with canopy cover and preferential selection for young stands in preference to pole-stage or mature stands (Welch et al., 1990). We predicted that with increasing canopy cover, lower light penetrance would have a negative effect on understory vegetation, thus reducing available food and therefore habitat use by roe deer. However, our finding that roe deer prefer small forests surrounded by arable land, coupled with our finding that there is higher roe deer use in forests with greater tree density and therefore higher canopy closure could suggest that roe deer are using forests more for shelter and feeding in nearby forest-agricultural ecotones during spring and summer months (Mysterud, 1996; Rigoudy et al., 2024) . This could be further investigated by analysing the temporal activity patterns of roe deer within forests, either by classification of behavioural states (e.g., feeding, moving, resting) from trail camera images and/or from deer habitat selection studies (Marshall et al., 2026b).

Despite several studies finding an effect of deciduous cover on roe deer habitat use (Zorzi et al., 2022; Ramirez et al., 2023; Schwegmann et al., 2023), our study did not detect this. This could be because of other local forest habitat variables, e.g., tree species richness, that capture similar information. As our study focused on variation in deer use at finer spatial scales (i.e., at the deployment level), local deployment habitat characteristics may have stronger explanatory power than the forest-scale habitat variables we used in the analysis. The effect of deciduous cover may become more apparent when analysing roe deer habitat use at broader patch or landscape scales (Jackson, 2000; Holland, Bert & Fahrig, 2004; Jackson & Fahrig, 2014; Heit et al., 2023). Also, as mentioned above, roe deer could be using forests more for shelter in this landscape, and foraging outside of forests during the spring to autumn survey period of this study. For shelter, forests with higher coniferous cover and less foraging opportunities could be as suitable as deciduous forests.

Our focus on structural forest components in this study may have been most relevant to behaviour related to shelter, but not to feeding. Therefore, collection of habitat features related to feeding behaviour, including the ground flora and woody species composition (and thus forage quality) would be a valuable extension of this study. If roe deer are foraging mainly outside of forests during spring and summer months, then the quality of forage within the forest at this time of year may only be a minor factor in their habitat use. However, depending on the cropping regime in the wider landscape, it is possible that they would forage more in forest during the winter. If this is the case, then overall impact of roe deer on forests could be higher than suggested by the data available. This could be assessed in future studies by carrying out a woodland herbivore impact assessment in early spring (Armstrong et al., 2025) which would indicate the net impact of deer over the whole year.

4.3 Effects of human recreational use on roe deer habitat use

In line with our third prediction P3, we found that forests were used more by roe deer if they were used less frequently by humans. However, in contrast to previous studies of deer in more urbanised environments (Gandy et al., 2026), we did not find an effect of the amount of urban area in the landscape surrounding forest patches on roe deer forest use. This was likely due to the low overall proportion of this land cover type in the landscape, and limited variation between sites. A negative effect of human activity within forest patches on roe deer habitat use is likely to be a direct effect of human disturbance, consistent with previous studies showing that deer reduce space use near areas of human activity such as trails (Mols et al., 2022a,b). This effect could also occur if forest characteristics that are attractive to humans are unattractive to deer due to differences in habitat, though this is considered very unlikely at our study sites since almost all forests were mixed, multi-use forests. Our measure of human usage of the forests would have underestimated recreational use of forests due to placement of cameras to avoid trails; however, this method was consistent across all forest patches so is unlikely to cause bias. It could be argued that our measure of human forest use, which was of humans walking away from trails, may be more likely to be relevant to disturbance of deer. Our results are consistent with previous studies which have shown that recreational use of trails within forests impacts space use by deer at a fine scale of between 20-200m within forests. This is extremely relevant to the disservices rendered by roe deer since this published work also shows that roe deer habitat use can also have cascading effects on the distribution of *Ixodes ricinus* ticks which are hosted by deer (Mols et al., 2022a).

4.4 Limitations

In terms of generalisability, previous studies which investigate landscape and forest drivers of roe deer habitat utilisation have found that effects can be context specific, depending on the interaction of multiple factors at multiple spatial scales, including climate, deer density, forage availability, land cover type and relative densities of other deer species. Therefore, the results from our study are likely to be specific to habitat use in a lowland agricultural-forest mosaic. Habitat use in different environments – e.g., in areas dominated by forestry, or open upland landscapes with fragmented forest – are likely to be different and highlight the need to examine deer habitat use within specific landscapes to better inform land use and forest management.

We did not have access to hunting pressure in the forests used in this study. Hunting effort in Scotland is determined by landowners and targets agreed under local deer management plans. Depending on cull intensity, this can influence population density and forest roe deer usage, and can also influence functional connectivity (Bonnot et al., 2013; Martin et al., 2018). Therefore, hunting pressure would be an important factor to measure within the forest and surrounding landscape in future studies.

Our statistical models explained 27% of the total variation in roe deer encounter rates likely due to explanatory factors we did not measure, including habitat characteristics at finer spatial scales (e.g., vegetation type at the camera location) as well as the effects of deer and forest management. Moreover, random effects had more explanatory power compared to fixed effects which explained only 10% of the total variation in roe deer encounter rates which may suggest the importance of unmeasured within-forest or landscape factors, or temporal effects (e.g., seasonal changes in roe deer forest use).

4.5 Management implications

Scotland and other European countries are undergoing significant forest expansion, (Forestry Europe, 2020). Our research suggests that patterns of forest and surrounding agricultural land use by roe deer and associated impacts will change with forest expansion if these result in changes in forest configuration. In this section we highlight how this knowledge can be used to inform deer monitoring and management within the current forest-agricultural mosaic landscape and within forest creation schemes to avoid increasing negative impacts.

Results of this study could be useful for land and forest managers to develop targeted monitoring for disservices to underpin deer management. For example, managers may consider monitoring for disservices such as herbivory impacts, biodiversity assessment, and assessing the hazard to humans from the tick vector *Ixodes ricinus*, which transmits the bacteria causing Lyme disease in people in areas predicted to have higher roe deer usage; e.g., in smaller, more connected forest patches and within forest edge and ecotonal areas of forest patches. Predicted patterns of roe deer forest use can also be used to understand where impacts to surrounding agricultural crops are likely to be highest, and identify the areas of highest overlap of deer and livestock pasture use, which could lead to increased environmental parasite and pathogen transmission. For example, risks to livestock from the tick *I. ricinus* have been shown to be higher on pastures adjacent to more woodland (Gilbert et al., 2017) and this might be expected to be even more of an issue in areas of higher deer populations due to deer transporting ticks from forest to pasture (Ruiz-Fons & Gilbert, 2010). This tick vector transmits a number of bacterial, viral and protozoal pathogens which can cause high mortality and morbidity in cattle and sheep (Böhm et al., 2007; Mitchell, 2019; Johnson et al., 2022).

Within forest creation schemes, this research could be used strategically to develop of land manager guidelines to monitor and mitigate a range of disservices linked to deer populations. For example, land managers may wish to incorporate habitat features that may be attractive to deer, such as edges, gaps or rides, so that deer controllers might more effectively focus their culling activities, or incorporate associated infrastructure such as high seats and hides. Apparent preference of roe deer for edge habitats, suggest that browsing impacts may be greatest in this zone, and forest managers may wish to design forest patches to maximise interior areas and thus limit browsing. Identifying where forest expansion schemes are likely to attract roe deer populations, may also be helpful in pre-empting where impacts to surrounding agricultural crops are likely to increase. As well as implications for damage to forestry, changing habitat use patterns could have important future consequences for humans if this overlaps with human activities resulting in greater risks from ticks in the environment, or greater risks from road traffic collisions (Joys, Fuller & Dolman, 2004; Böhm et al., 2007; Gill & Fuller, 2007; Gilbert et al., 2012; Nelli et al., 2018).

Finally, this study demonstrates the use of camera traps and publicly available AI models in quantifying the utilisation of forest habitats by deer of relevance to management practitioners. Camera-traps provide non-invasive and more direct means of estimating habitat use and abundance of species of interest compared to indirect dung counts, with relatively low cost and effort compared to other methods such as GPS tracking or thermal imaging using Unmanned Aerial Vehicles (UAV). Because cameras can be deployed for long periods of time with minimal supervision, they can also be used to monitor population changes over time or in response to management efforts. Moreover, the availability of free and open-source image management software combined with shared image repositories e.g., Wildlife Insights (Ahumada et al., 2020) and MammalWeb (Hsing et al., 2022) allow for efficient processing of images and faster extraction of estimates – such as population density or relative abundance, in an accessible manner to non-expert practitioners.

5 Acknowledgements

This research forms part of the TickSolve project (https://ticksolve.ceh.ac.uk/) and was funded by UK Research and Innovation through the NERC grant funding; NE/W003244/1 NE/W003171/1, and NE/W003260/1. For permission to conduct the work, we thank land-owners for allowing us to access their land. We would also like to thank all field volunteers for their help with camera deployment.

5.1 Data and Software Statement

The data and R script used for analysis in this manuscript have been made available at DOI: https://doi.org/10.5281/zenodo.18951596 Venkatesan et al. (2026). The files currently have restricted access but will be made publicly available on publication of the manuscript.

Data used by Marshall et al. (2026a) and here to generate functional connectivity estimates is available at: https://doi.org/10.5281/zenodo.18699745 (Marshall et al., 2026a).

Code used to generate functional connectivity estimates is available at: https://github.com/BenMMarshall/TICKSOLVE_DeerMovement; and archived at: https://doi.org/10.5281/zenodo.18701055 (Marshall, 2026).

A complete list of software used can be found in Appendix A1.7.

5.2 Author Contributions

Saudamini Venkatesan: Data curation, formal analysis, investigation, methodology, project administration, validation, visualisation, writing – original draft, writing – review and editing; Benjamin Marshall: Data curation, formal analysis, visualisation, writing – original draft, writing – review and editing; Mark Greener: Data curation, investigation, methodology, project administration; Anna Kinghorn: Methodology, validation; Isla Sligo-Young: Formal analysis, validation; Richard Hassall: Methodology Robin Gill: Writing – review and editing; Ben McKeown: Writing – review and editing; Jeanette Hall: Writing – review and editing; Roman Biek: Funding acquisition, project administration, resources; Lucy Gilbert: Conceptualisation, data curation, funding acquisition, investigation, methodology, project administration, resources, writing – review and editing; Tom Morrison: Conceptualisation, formal analysis, funding acquisition, investigation, methodology, project administration, resources, supervision, writing – review and editing; Caroline Millins (corresponding author): Conceptualisation, formal analysis, funding acquisition, investigation, methodology, project administration, resources, supervision, writing – original draft, writing – review and editing.

6 References

Abbas F, Morellet N, Hewison AJM, Merlet J, Cargnelutti B, Lourtet B, . . . Verheyden H. 2011. Landscape fragmentation generates spatial variation of diet composition and quality in a generalist herbivore. *Oecologia* 167:401–411. DOI: 10.1007/s00442-011-1994-0.

Ahumada JA, Fegraus E, Birch T, Flores N, Kays R, O'Brien TG, . . . Dancer A. 2020. Wildlife insights: A platform to maximize the potential of camera trap and other passive sensor wildlife data for the planet. *Environmental Conservation* 47:1–6. DOI: 10.1017/S0376892919000298.

Armstrong H, Thompson R, Holl K, Black B. 2025.Woodland herbivore impact assessment. *Available at https://www.forestry.gov.scot/publications/woodland-herbivore-impact-assessment-method-user-guide*

Bender DJ, Tischendorf L, Fahrig L. 2003. Using patch isolation metrics to predict animal movement in binary landscapes. *Landscape Ecology* 18:17–39. DOI: 10.1023/A:1022937226820.

Bjorneraas K, Solberg EJ, Herfindal I, Van Moorter B, Rolandsen CM, Tremblay JP, . . . Astrup R. 2011. Moose habitat use at multiple temporal scales in a human-altered landscape. *Wildlife Biology* 17:44–54. DOI: 10.2981/10-073.

Bobrowski M, Gillich B, Stolter C. 2020. Nothing else matters? Food as a driving factor of habitat use by red and roe deer in winter? *2020(4)* wlb.00723-wlb.00723. DOI: 10.2981/wlb.00723.

Böhm M, White PCL, Chambers J, Smith L, Hutchings MR. 2007. Wild deer as a source of infection for livestock and humans in the UK. *The Veterinary Journal* 174:260–276. DOI: 10.1016/J.TVJL.2006.11.003.

Bolker BM, Brooks ME, Clark CJ, Geange SW, Poulsen JR, Stevens MHH, White JSS. 2009. Generalized linear mixed models: A practical guide for ecology and evolution. *Trends in Ecology & Evolution* 24:127–135. DOI: 10.1016/J.TREE.2008.10.008.

Bonnot N, Morellet N, Verheyden H, Cargnelutti B, Lourtet B, Klein F, Hewison AJM. 2013. Habitat use under predation risk: Hunting, roads and human dwellings influence the spatial behaviour of roe deer. *European Journal of Wildlife Research* 59:185–193. DOI: 10.1007/s10344-012-0665-8.

Brooks ME, Kristensen K, Benthem KJ van, Magnusson A, Berg CW, Skaug AN, . . . Bolker BM. 2017. glmmTMB balances speed and flexibility among packages for zero-inflated generalized linear mixed modeling. *The R Journal* 9:378–400. DOI: 10.32614/RJ-2017-066.

Brown JS, Laundré JW, Gurung M. 1999. The ecology of fear: Optimal foraging, game theory, and trophic interactions. *Journal of Mammalogy* 80:385–399. DOI: Doi.

Ciach M, Fröhlich A. 2019. Ungulates in the city: Light pollution and open habitats predict the probability of roe deer occurring in an urban environment. *Urban Ecosystems* 22:513–523. DOI: 10.1007/s11252-019-00840-2.

Côté SD, Rooney TP, Tremblay JP, Dussault C, Waller DM. 2004. Ecological impacts of deer overabundance. Annual review of ecology, evolution, and systematics. *35(Volume* 35:113–147. DOI: 10.1146/annurev.ecolsys.35.021103.105725.

DEFRA. 2018.A green future: Our 25 year plan to improve the environment. *Available at https://assets.publishing.service.gov.uk/media/65fd713d65ca2f00117da89e/CD1.H_HM_Government_A_Green_Future_Our_25_Year_Plan_to_Improve_the_Environment.pdf* (accessed February 12, 2026).

Dickinson ER, Millins C, Biek R. 2020. Sampling scale and season influence the observed relationship between the density of deer and questing ixodes ricinus nymphs. *Parasites and Vectors* 13:1–11. DOI: 10.1186/S13071-020-04369-8.

Feng H, Li Y, Li Y, Li N, Li Y, Hu Y, . . . Luo H. 2021. Identifying and evaluating the ecological network of siberian roe deer (capreolus pygargus) in tieli forestry bureau, northeast China. *Global Ecology and Conservation* 26:e01477. DOI: 10.1016/j.gecco.2021.e01477.

Forestry Commission. 2019.National forest inventory woodland map 2019 (GB) [data set]. *Available at https://www.data.gov.uk/dataset/4f73f738-5c3f-4b40-8a8e-0ccae715de2f/national-forest-inventory-woodland-map-2019-gb*

Forestry Europe. 2020.State of europe's forests: 2020. Forest europe liaison unit bratislava. *Available at https://foresteurope.org/wp-content/uploads/2016/08/SoEF_2020.pdf* (accessed February 12, 2026).

Fuentes-Montemayor E, Ferryman M, Watts K, Macgregor NA, Hambly N, Brennan S, . . . Park KJ. 2020. Small mammal responses to long-term large-scale woodland creation: The influence of local and landscape-level attributes. *Ecological Applications* 30:e02028. DOI: 10.1002/eap.2028.

Fuller RJ, Gill RMA. 2001. Ecological impacts of increasing numbers of deer in british woodland. *Forestry: An International Journal of Forest Research* 74:193–199. DOI: 10.1093/FORESTRY/74.3.193.

Gandy SL, Hall J, Plahe G, Johnson D, Birtles R, Gilbert L. 2026. Temporal and spatial drivers of lyme disease hazard differ between urban and rural environments. *Landscape and Urban Planning* 269:105597. DOI: 10.1016/j.landurbplan.2026.105597.

Gilbert L, Brunker K, Lande U, Klingen I, Grøva L. 2017. Environmental risk factors for ixodes ricinus ticks and their infestation on lambs in a changing ecosystem: Implications for tick control and the impact of woodland encroachment on tick-borne disease in livestock. *Agriculture, Ecosystems & Environment* 237:265–273. DOI:

10.1016/J.AGEE.2016.12.041.

Gilbert L, Maffey GL, Ramsay SL, Hester AJ. 2012. The effect of deer management on the abundance of ixodes ricinus in scotland. *Ecological Applications* 22:658–667. DOI: 10.1890/11-0458.1.

Gill RMA, Fuller RJ. 2007. The effects of deer browsing on woodland structure and songbirds in lowland britain. *Ibis* L:119–127. DOI: 10.1111/J.1474-919X.2007.00731.

Gill RMA, Johnson AL, Francis A, Hiscocks K, Peace AJ. 1996. Changes in roe deer (capreolus capreolus l.) population density in response to forest habitat succession. *Forest Ecology and Management* 88:31–41. DOI: 10.1016/S0378-1127(96)03807-8.

Hanski I. 1998. Metapopulation dynamics. *Nature* 1998:396. DOI: 10.1038/23876.

Hartig F. 2022. *DHARMa: Residual diagnostics for hierarchical (multi-level / mixed) regression models*. In.

Heit DR, Millspaugh JJ, McRoberts JT, Wiskirchen KH, Sumners JA, Isabelle JL, . . . Moll RJ. 2023. The spatial scaling and individuality of habitat selection in a widespread ungulate. *Landscape Ecology* 38:1481–1495. DOI: 10.1007/S10980-023-01631-Z.

Hewison AJM, Vincent JP, Joachim J, Angibault JM, Cargnelutti B, Cibien C. 2001. The effects of woodland fragmentation and human activity on roe deer distribution in agricultural landscapes. *Canadian Journal of Zoology* 79:679–689. DOI: 10.1139/Z01-032.

Hill DA. 2005. *Handbook of biodiversity methods: Survey, evaluation and monitoring*.

Hofmeester TR, Marcus Rowcliffe J, Jansen PA. 2017. Quantifying the availability of vertebrate hosts to ticks: A camera-trapping approach. *Frontiers in Veterinary Science* 4. DOI: 10.3389/fvets.2017.00115.

Holland JD, Bert DG, Fahrig L. 2004. Determining the spatial scale of species' response to habitat. *BioScience* 54:227–233. DOI: 10.1641/0006-3568(2004)054[0227:dtssos]2.0.co;2.

Hsing P-Y, Hill RA, Smith GC, Bradley S, Green SE, Kent VT, . . . Stephens PA. 2022. Large-scale mammal monitoring: The potential of a citizen science camera-trapping project in the united kingdom. *Ecological Solutions and Evidence* 3:e12180. DOI: 10.1002/2688-8319.12180.

Jackson DL. 2000.Guidance on the interpretation of the biodiversity broad habitat classification (terrestrial and freshwater types): Definitions and the relationship with other habitat classifications. *Available at http://www.jncc.gov.uk/page-2433*

Jackson H, Fahrig L. 2014. Are ecologists conducting research at the optimal scale? *Global Ecology and Biogeography* 24. DOI: 10.1111/geb.12233.

Johnson N, Phipps LP, Hansford KM, Folly AJ, Fooks AR, Medlock JM, Mansfield KL. 2022. One health approach to tick and tick-borne disease surveillance in the united kingdom. *International Journal of Environmental Research and Public Health* 19:5833. DOI: 10.3390/ijerph19105833.

Joys AC, Fuller RJ, Dolman PM. 2004. Influences of deer browsing, coppice history, and standard trees on the growth and development of vegetation structure in coppiced woods in lowland england. *Forest Ecology and Management* 202:23–37. DOI: 10.1016/J.FORECO.2004.06.035.

Linard C, Lamarque P, Heyman P, Ducoffre G, Luyasu V, Tersago K, . . . Lambin EF. 2007. Determinants of the geographic distribution of puumala virus and lyme borreliosis infections in belgium. *International Journal of Health Geographics* 6:1–14. DOI: 10.1186/1476-072X-6-15.

Loro M, Ortega E, Arce RM, Geneletti D. 2016. Assessing landscape resistance to roe deer dispersal using fuzzy set theory and multicriteria analysis: A case study in central spain. *Landscape and Ecological Engineering* 12:41–60. DOI: 10.1007/s11355-015-0275-1.

Lovari S, Serrao G, Mori E. 2017. Woodland features determining home range size of roe deer. *Behavioural Processes* 140:115–120. DOI: 10.1016/J.BEPROC.2017.04.012.

Lüdecke D, Ben-Shachar MS, Patil I, Waggoner P, Makowski D. 2021. Performance: An r package for assessment, comparison and testing of statistical models. *Journal of Open Source Software* 6:3139. DOI: 10.21105/joss.03139.

Lush MJ, Lush CE. 2026.Deer vehicle collision analysis 2022-2024. *Available at https://www.nature.scot/professional-advice/land-and-sea-management/managing-wildlife/deer-scotland/deer-vehicle-collisions*

Marshall BM. 2026. *BenMMarshall/TICKSOLVE_DeerMovement: 0.9.1 preprint (0.9.1)*. Zenodo. DOI: 10.5281/zenodo.18701056.

Marshall B, Gilbert L, Bolye J, Lhamine V, Greener M, others, Morrison T. 2026a. *Supporting data for roe deer show an affinity for woodland and reluctance to cross roads (0.9.1) [data set]*. Zenodo. DOI: 10.5281/zenodo.18699746.

Marshall BM, Gilbert L, Boyle J, Lhamine VV, Greener MS, others, Morrison TA. 2026b. Roe deer show an affinity for woodland and reluctance to cross roads. *EcoEvoRix*. DOI: 10.32942/X2JD47.

Marston C, Rowland CS, O'Neil AW, Morton RD. 2022. Land cover map 2021 (25m rasterised land parcels, GB). In: *NERC EDS environmental information data centre*.

Martin J, Vourc'h G, Bonnot N, Cargnelutti B, Chaval Y, Lourtet B, . . . Morellet N. 2018. Temporal shifts in landscape connectivity for an ecosystem engineer, the roe deer, across a multiple-use landscape. *Landscape Ecology* 33:937–954. DOI: 10.1007/S10980-018-0641-0.

Mason SS, Hill RA, Whittingham MJ, Cokill J, Smith GC, Stephens PA. 2022. Camera trap distance sampling for terrestrial mammal population monitoring: Lessons learnt from a UK case study. *Remote Sensing in Ecology and Conservation* 8:717–730. DOI: 10.1002/rse2.272.

Mitchell S. 2019. Surveillance for disease in extensively managed livestock. *Veterinary Record* 185:686–687. DOI: 10.1136/vr.l6843.

Mols B, Churchill JE, Cromsigt JPGM, Kuijper DPJ, Smit C. 2022a. Recreation reduces tick density through fine-scale risk effects on deer space-use. *Science of The Total Environment* 839:156222–156222. DOI: 10.1016/J.SCITOTENV.2022.156222.

Mols B, Lambers E, Cromsigt JPGM, Kuijper DPJ, Smit C. 2022b. Recreation and hunting differentially affect deer behaviour and sapling performance. *Oikos* 2022. DOI: 10.1111/oik.08448.

Morellet N, Moorter B van, Cargnelutti B, Angibault JM, Lourtet MB, Merlet J, . . . Hewison AJM. 2011. Landscape composition influences roe deer habitat selection at both home range and landscape scales. *Landscape Ecology* 26:999–1010. DOI: 10.1007/S10980-011-9624-0.

Morton D, Marston CG, O'Neil AW, Rowland CS. 2024. Land cover map 2023 (25m rasterised land parcels, GB). In: *NERC EDS environmental information data centre*.

Mysterud A. 1996. Bed-site selection by adult roe deer capreolus capreolus in southern norway during summer. *Wildlife Biology* 2:101–106. DOI: 10.2981/wlb.1996.038.

Mysterud A, Easterday WR, Stigum VM, Aas AB, Meisingset EL, Viljugrein H. 2016. Contrasting emergence of lyme disease across ecosystems. *Nature Communications* 7. DOI: 10.1038/ncomms11882.

Mysterud A, Lian L-B, Hjermann DØ. 1999. Scale-dependent trade-offs in foraging by european roe deer (capreolus capreolus) during winter. *Canadian journal of zoology* 77:1486–1493. DOI: 10.1139/z99-118.

NatureScot. 2016.Deer management in scotland: Report to the scottish government from scottish natural heritage 2016. *Available at https://www.nature.scot/doc/archive/deer-management-scotland-report-scottish-government-scottish-natural-heritage*

NatureScot. 2025.The proportion of protected sites in favourable condition 2025. *Available at https://www.nature.scot/doc/proportion-scotlands-protected-sites-favourable-condition-2025* (accessed February 12, 2026).

Nelli L, Langbein J, Watson P, Putman R. 2018. Mapping risk: Quantifying and predicting the risk of deer-vehicle collisions on major roads in england. *Mammalian Biology* 91:71–78. DOI: 10.1016/J.MAMBIO.2018.03.013.

Noble DG, Aebischer NJ, Newson SE, Ewald D J. A. Dadam. 2012. A comparison of trends and geographical variation in mammal abundance in the breeding bird survey and the national gamebag census.

Ordnance Survey. 2024. OS open roads v. 2.4.

Panzacchi M, Van Moorter B, Strand O, Saerens M, Kivimäki I, St. Clair CC, . . . Boitani L. 2016. Predicting the continuum between corridors and barriers to animal movements using step selection functions and randomized shortest paths. *Journal of Animal Ecology* 85:32–42. DOI: 10.1111/1365-2656.12386.

Pfeffer SE, Spitzer R, Allen AM, Hofmeester TR, Ericsson G, Widemo F, . . . Cromsigt JPGM. 2018. Pictures or pellets? Comparing camera trapping and dung counts as methods for estimating population densities of ungulates. *Remote Sensing in Ecology and Conservation* 4:173–183. DOI: 10.1002/rse2.67.

Posit team. 2024. *RStudio: Integrated development environment for r*. Boston, MA: Posit Software, PBC.

Putman R, Langbein J, Green P, Watson P. 2011. Identifying threshold densities for wild deer in the UK above which negative impacts may occur. *Mammal Review* 41:175–196. DOI: 10.1111/j.1365-2907.2010.00173.x.

Putman RJ, Moore NP. 1998. Impact of deer in lowland britain on agriculture, forestry and conservation habitats. *Mammal Review* 28:141–164. DOI: 10.1046/J.1365-2907.1998.00031.X.

R. Core Team. 2024. *R: A language and environment for statistical computing*. Vienna, Austria: R Foundation for Statistical Computing.

Ramirez JI, Poorter L, Jansen PA, Ouden J den, Siewert M, Olofsson J. 2023. Top-down and bottom-up forces explain patch utilization by two deer species and forest recruitment. *Oecologia* 201:229–240. DOI: 10.1007/S00442-022-05292-8.

Rigoudy N, Chamaillé-Jammes S, Hewison AJM, Bonnet A, Chaval Y, Lourtet B, . . . Morellet N. 2024. Crop phenology reshapes the food-safety landscape for roe deer in an agroecosystem. *Journal of Applied Ecology* 61:564–574. DOI: 10.1111/1365-2664.14581.

Rizzoli A, Hauffe HC, Tagliapietra V, Neteler M, Rosà R. 2009. Forest structure and roe deer abundance predict tick-borne encephalitis risk in italy. *PLOS ONE* 4:e4336–e4336. DOI: 10.1371/JOURNAL.PONE.0004336.

Ruiz-Fons F, Gilbert L. 2010. The role of deer as vehicles to move ticks, ixodes ricinus, between contrasting habitats. *International Journal for Parasitology* 40:1013–1020. DOI: 10.1016/j.ijpara.2010.02.006.

Saïd S, Servanty S. 2005. The influence of landscape structure on female roe deer home-range size. *Landscape Ecology* 20:1003–1012. DOI: 10.1007/S10980-005-7518-8.

Scholefield PA, Morton RD, Rowland CS, Henrys PA, Howard DC, Norton LR. 2016. Woody linear features framework. *Great Britain v* 1. DOI: 10.5285/D7DA6CB9-104B-4DBC-B709-C1F7BA94FB16.

Schwegmann S, Hendel AL, Frey J, Bhardwaj M, Storch I. 2023. Forage, forest structure or landscape: What drives roe deer habitat use in a fragmented multiple-use forest ecosystem? *Forest Ecology and Management* 532:120830–120830. DOI: 10.1016/J.FORECO.2023.120830.

Scottish Government. 2019.Scotland's forestry strategy. *Available at https://www.gov.scot/publications/scotlands-forestry-strategy-20192029/* (accessed February 12, 2026).

Scottish Government. 2024.Scottish biodiversity delivery plan 2024-2030. *Available at https://www.gov.scot/publications/scottish-biodiversity-delivery-plan-20242030/* (accessed February 12, 2026).

Spake R, Bellamy C, Gill R, Watts K, Wilson T, Ditchburn B, Eigenbrod F. 2020. Forest damage by deer depends on cross-scale interactions between climate, deer density and landscape structure. *Journal of Applied Ecology* 57:1376–1390. DOI: 10.1111/1365-2664.13622.

Torres RT, Carvalho JC, Panzacchi M, Linnell JDC, Fonseca C. 2011. Comparative use of forest habitats by roe deer and moose in a human-modified landscape in southeastern norway during winter. *Ecological Research* 26:781–789. DOI: 10.1007/S11284-011-0837-0.

Torretta E, Ruffoni G, Bergantin E, Frigerio E. 2025. *Balancing risk: The influence of human disturbance and predators on roe deer activity patterns*. Current Zoology. DOI: 10.1093/cz/zoaf048.

Venkatesan S, Marshall B, Greener M, Anna K, Isla S-Y, Biek R, Gilbert L, Morrison T, Millins C. 2026. Supporting data for drivers of roe deer use in fragmented forest landscapes; implications for management in the context of policy driven forest expansion. DOI: 10.5281/zenodo.18951596.

Wearn OR, Glover-Kapfer P. 2019. Snap happy: Camera traps are an effective sampling tool when compared with alternative methods. *R Soc Open Sci* 6:181748. DOI: 10.1098/rsos.181748.

Welch D, Staines BW, Catt DC, Scott D. 1990. Habitat usage by red (cervus elaphus) and roe (capreolus capreolus) deer in a scottish sitka spruce plantation. *Journal of Zoology* 221:453–476. DOI: 10.1111/j.1469-7998.1990.tb04013.x.

Zorzi P, Nardotto A, Bottazzo M, Dal Zotto M. 2022. Habitat selection of the roe deer capreolus capreolus (artiodactyla: Cervidae) in an agroforestry system. *Natural History Sciences* 9:3–6. DOI: 10.4081/nhs.2022.550.

Zuur AF, Ieno EN, Elphick CS. 2010. A protocol for data exploration to avoid common statistical problems. *Methods in Ecology and Evolution* 1:3–14. DOI: 10.1111/J.2041-210X.2009.00001.X.

Appendix

A1. Methods

A1.1. Forest selection

Forest selection and extraction of variables were carried out in R using packages raster (Hijmans, 2024a), and terra (Hijmans, 2024b). Forest patch selection was carried out as a part of the larger Ticksolve project (Venkatesan et al. in prep) across two different study landscapes within the UK. Forests were identified using the Land Cover Map 2021 (Marston et al., 2022) in conjunction with the National Forest Inventory (Forestry Commission, 2019) as contiguous areas of broadleaved and/or evergreen forest from a raster of 25m X 25m resolution. The area of every forest (km^2) was calculated using LCM 2021 by multiplying the number of cells comprising the forest by the area of a single cell. A structural forest connectivity metric was calculated using a distance weighted area-based metric (Bender et al., 2003; Hanski, 1998) as follows:

$$S_i = \sum_{j \neq i} A_j \exp\left(-d_{i,j}\right)$$

where the structural connectivity of the focal forest is determined by the area of patch *j* and the Euclidean distance between the focal forest *i* and forest *j* within a radius around the focal forest. For the purposes of site selection, we used 5 different radii (250m, 1.5km, 2km, 5km and 10km) to account for the home range of different deer species (fallow, roe and red deer; Gill & Morgan, 2010) across the two study landscapes and averaged the measures to obtain a single mean connectivity metric per forest patch. In order to facilitate site selection across a gradient of both forest patch size and connectivity, the patch size variable was divided into 5 quantiles, and the connectivity metric was divided in 2 quantiles (Figure A1.1). The final 30 forest patches were selected by sampling equally patch size and connectivity quantiles.

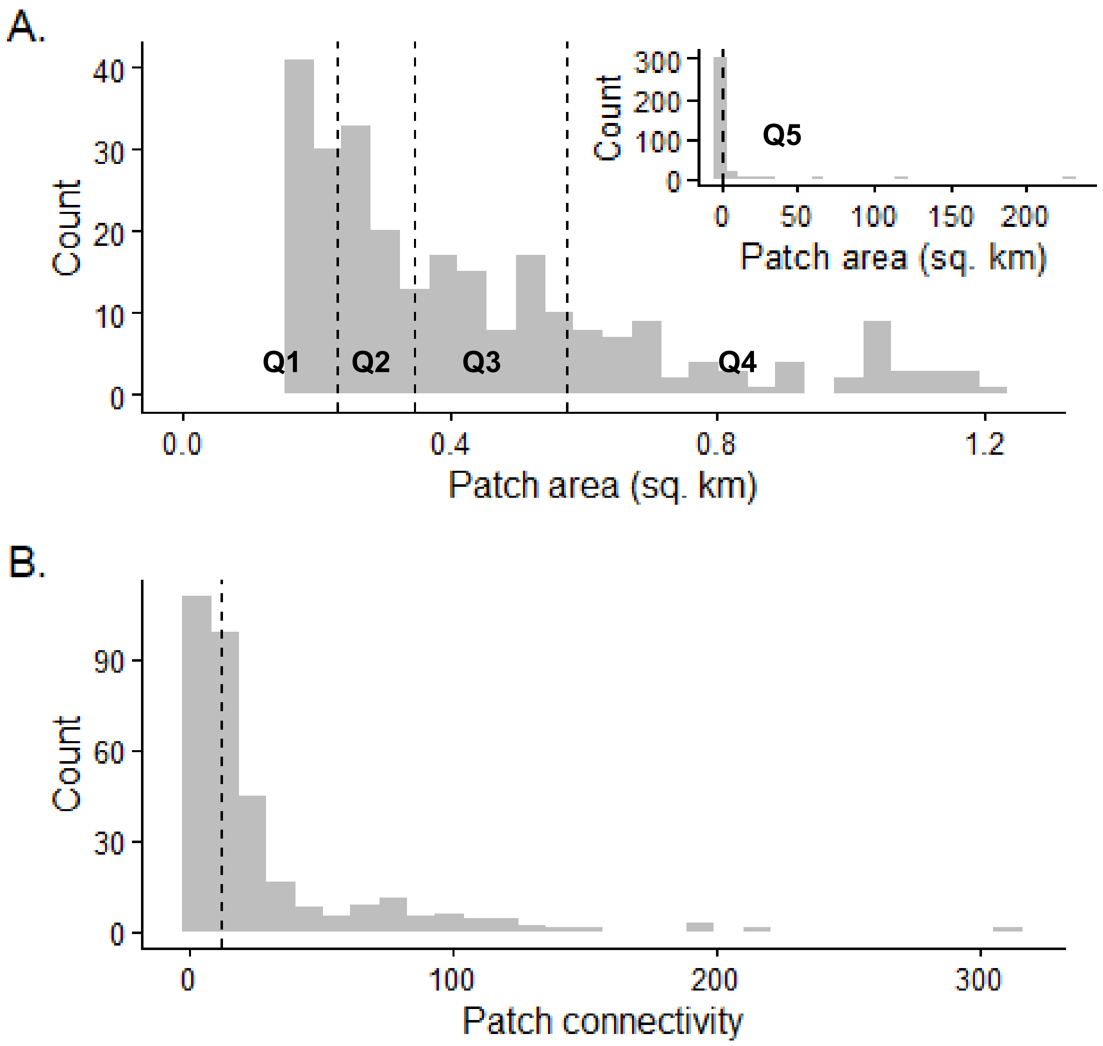

Figure A1.1: Histograms with frequency distribution of patch size (A) and connectivity (B) across all forest patches in the landscape. (A) Patch sizes were divided into 5 quantiles (dashed lines) – Q1 (0.16-0.22 km^2), Q2 (0.23-0.34 km^2), Q3 (0.35-0.57 km^2), Q4 (0.58-1.24 km^2) and Q5 (inset)(1.25-228 km^2). (B) Patch connectivity was divided into two quantiles (dashed lines) – Below Median (3.46-12.72) and Above Median (12.73-311.0). The final 30 forest patches in this study were chosen by sampling equally across these categories.

A1.2. Landscape variables

Forest patch area and structural connectivity used for analyses in this manuscript were re-calculated using more recent Land Cover Map 2023 (Morton et al., 2024). For structural connectivity, we used the formula described in Section A1.1 and a radius of 750m, reflecting the home range of the dominant deer species – roe deer in Aberdeenshire. To calculate the proportion of major land use classes around the forest, LCM 2023 Land Cover classes (Morton et al., 2024) were merged to obtain four broad land use classes - Forest, Arable, Grassland and Urban (Table A1.1). Proportions of each major class was then calculated by taking a proportion of the cells with the specific land cover class to the total number of cells in a 750m buffer around the forest patch. Forest edge density was calculated by estimating length of forest edges in a 750m buffer around focal forest patch and dividing by the area of the buffer. Finally, for every camera deployment we obtained the distance to edge of forest by estimating the Euclidean distance between the deployment coordinates and the closest edge of the forest where the camera was deployed using QGIS (v.3.40.2) (Quantum GIS Development Team, 2025).

Table A1.1*: Grouping of LCM 2023 (Morton et al., 2024) land cover classes into broader land use categories used to calculate the "Proportion land use" variable described in Table 1. Multiple LCM classes were combined to derive broader ecologically relevant land use classifications.*

Land Use Class	LCM 2023 Land Cover Class
Forest	Deciduous forest
	Coniferous forest
Arable	Arable
Grassland	Improved grassland
	Neutral grassland
	Calcareous grassland
	Acid grassland
	Heather
	Heather grassland

Urban	Urban
	Suburban

A1.3. Estimating roe deer functional connectivity

We took the estimates of habitat preference, and movement interactions with land types estimated by the Poisson population level from Marshall et al. (2026a). We mapped these estimates of selection for the land cover types, and effect for all the environmental aspects of interest (i.e., roads and hedgerows; Ordnance Survey, 2024; Scholefield et al., 2016) back onto the landscape, resulting in a map of conductance (Fig A1.2). This process took the form of generating a model matrix based on all environmental covariates at each cell in the overall landscape raster and using the fitted Poisson model coefficients to calculate predicted deer use for each cell. For roads we rasterised the road polyline data and used the road crossing coefficient to create a conductance value for the road cells. For the covariates that involved movement interactions, we used the mean step and turn angle in calculations of predicted use. We replaced any areas with 0 conductance with 1e-12 to avoid any dead-ends or any absolute barriers. For these resistance maps, we ignored the uncertainty surrounding the selection estimates, instead relying on just the point estimates for the resistance mapping.

We used random shortest paths, that consists of generating random walks between locations, to simulate potential connectivity across the landscapes based on the above-described conductance/resistance raster. This method was previously used to show the connectivity of areas used by reindeer and offers a mechanism for calibrating the connectivity maps to both the habitat selection and movement path characteristics (Panzacchi et al., 2016).

We used forest patches as the sources of our random locations. We limited calculations of random shortest paths to pairs of patches that existed within 750 m of each other. We selected 750 m as that represented the mean longest axis of the 99% home range estimate of the deer (excluding outlying non-contiguous portions of the area polygons; Marshall et al., 2026a). For every pairing, we generated 6 start and end locations in each patch and ran random shortest paths between these locations. We repeated this for every pairing of patches. We elected not to generate start or end points in patches less than 0.5ha in areas, due to these patches being unlikely to host deer populations and the reduction in origin patches aided computational costs. The 0.5 ha threshold meant that 3415 Aberdeenshire patches were included in the generation of random shortest paths; thereby, necessitating optimisations for the sake of computing time. Instead of considering the entire landscape when calculating the paths, the vast majority of which would not play a role between two neighbouring patches, we cropped the conductance raster to only include the area surrounding the randomly selected start and end points. This cropped area was 750m in all directions from the start and end points; where start and end points exceeded four times 750m apart from each other we extended the cropped area to half the distance between the two points in all directions. This was required to avoid prohibitively computationally intensive paths (i.e., those that encompassed nearly the entire landscape) caused by patches with large areas. A further optimisation was required to run the random shortest paths efficiently; we limited the distance between start and end location to four times the mean longest axis of the 99% home range estimate (four times 756 m). The adaptive cropping and path length restrictions allowed for much faster calculation, while retaining sufficient raster landscape for circuitous paths to be estimated.

Once every walk was complete, the resulting rasters describing the likelihood of a deer crossing a cell are compiled into a single landscape raster describing connectivity and standardised between 0 and 1 (where 0 is low connectivity and 1 is high connectivity). For inclusion in statistical models, connectivity values across all cells within a forest patch polygon were averaged to obtain functional connectivity of the forest patches in our study.

A key consideration in these walks is how random/diffuse the paths are. We elected to run walks at 3 different levels of randomness (*theta*; with 1 being close to a least cost path, and 10^{-5} being the most random and diffuse walks; Fig. A1.3).

To determine what level of randomness best reflected the realised movements of the deer, we compared the resulting connectivity maps to dynamic Brownian Bridge Movement Models (Kranstauber et al., 2012; Kranstauber et al., 2024). Dynamic Brownian Bridge Movement Models run a series of random walks between defined start and end points; from the summation of these walks, you can extract a rasterised occurrence distribution. Critically the dBBMM walks are calibrated to the movement capacity of the animal through rolling window (i.e., a number of data points/known locations) that summarises the movement rate during that time. Additionally, within that window, a margin (a subset of data points) is used to detect any sudden changes in movement capacity that may be reflect of behavioural/movement mode changes. Therefore, the dBBMMs provide an estimate of how diffuse the movements could be between known locations. We ran dBBMMs using the previously reference roe deer movement data with a window size of 29 and a margin of 5. This provided estimates of motion variance on roughly a weekly sliding window with the allowance of sudden motion variance changes day to day (margin). We compared the dBBMMs to the connectivity maps constructed with varying levels of randomness (i.e., *theta*), and used mean squared error to determine which level of randomness best fit the movement data. We used the connectivity map created using that theta value for all subsequent analysis (*theta* of $1e^{-5}$; Fig. A1.3), extracting the mean cell connectivity value per patch and surrounding 750m buffer.

We examined whether the connectivity maps generated matched the observed movements of roe deer using a logistic model. The model was supplied with the known locations of deer as well as 10 randomly generated points per known deer location across the landscape, all of which had associated connectivity values. We formulated the model to predict whether a point was used or random based on the connectivity values, and we included a random effect for deer ID. The expectation was that the model coefficients would indicate that deer locations were positively associated with higher connectivity values; and the models support this (Fig. A1.4).

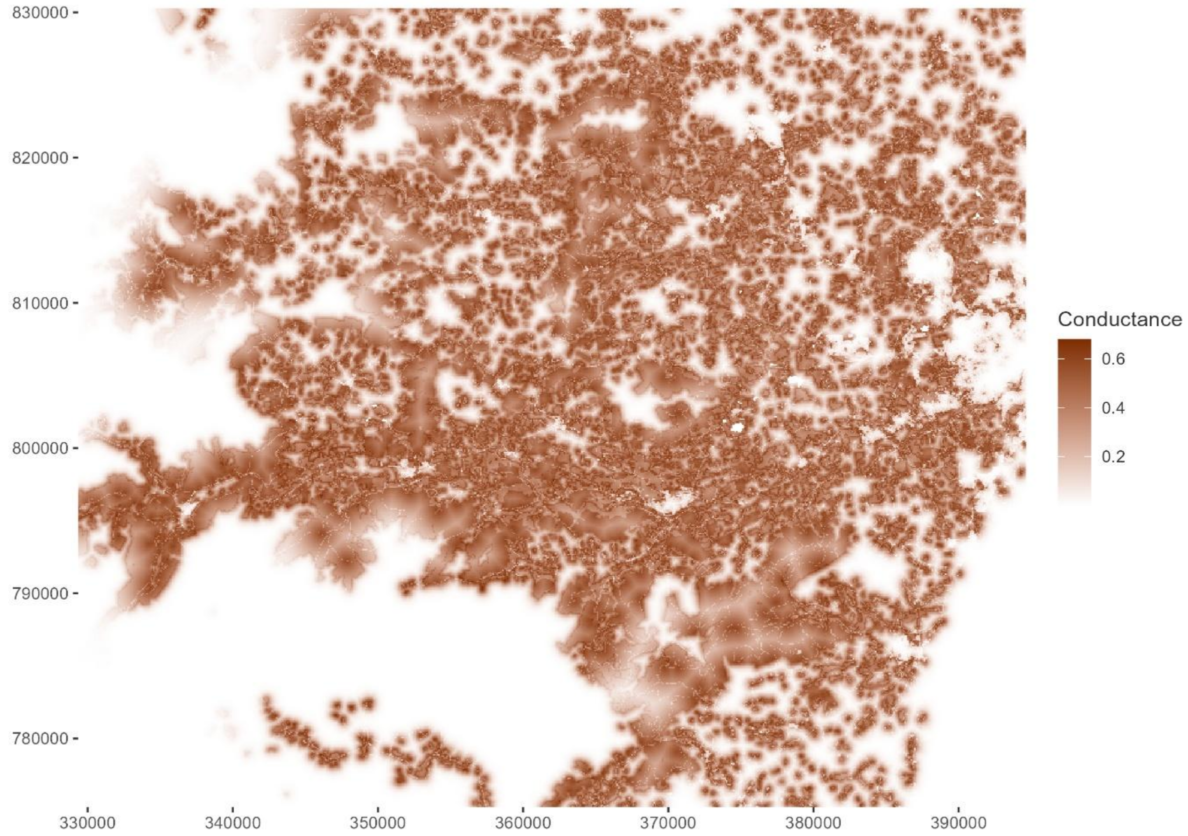

Fig. A1.2: Conductance map of Aberdeen landscape developed from the coefficients of the Poisson habitat selection model. Higher values indicate easier movement for Roe Deer. Axis are metres in British National Grid coordinate system.

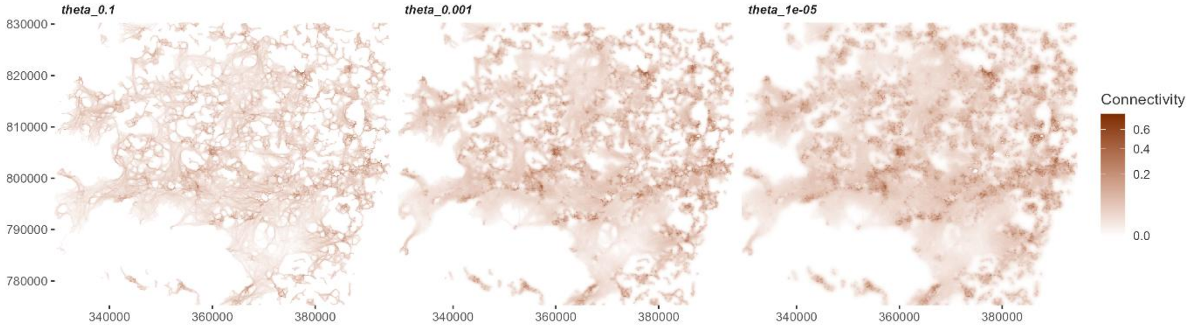

Fig A1.3: The connectivity maps under differing levels of theta (randomness) in the random shortest paths between patches. The colour scale is square-rooted to better differentiate low connectivity areas. Darker areas are suggestive of higher connectivity with more random paths existing in that cell. Axis are metres in British National Grid coordinate system.

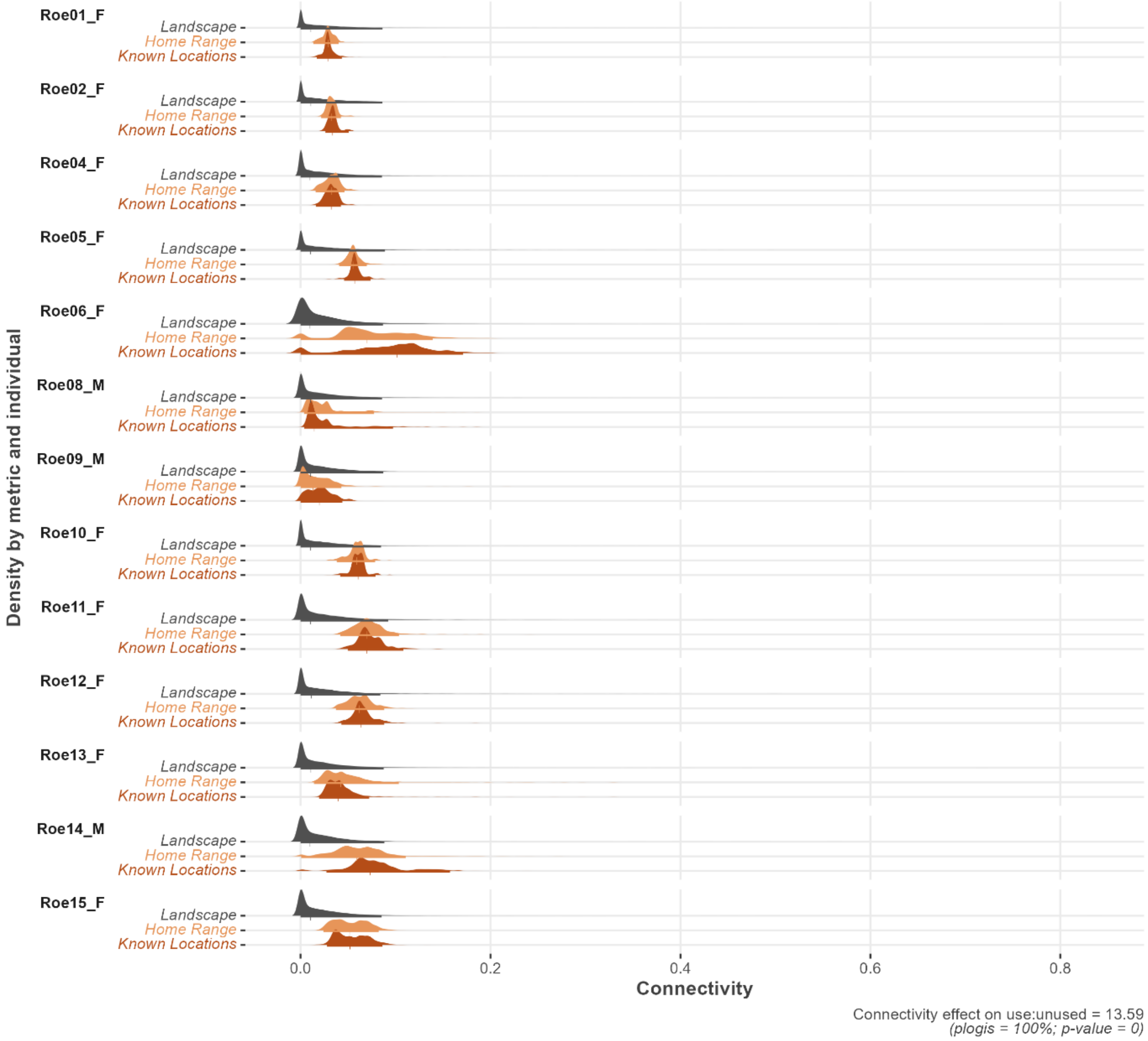

Fig A1.4: Distribution of connectivity values at known deer locations and randomly generated locations across the Aberdeen landscape, as well as random locations generated within the 95% home range. Lower caption describes the results of the logistic model testing whether connectivity can predict if the location was random or a known deer location.

A1.4. Distance between camera deployments

To ensure that distance between cameras did not increase significantly with increasing patch size and for logistical reasons, we deployed cameras in a smaller region within a forest patch in the 9 largest forest patches (> 80ha). Additionally, we estimated the mean and median distance between cameras in each patch by first calculating the Euclidean distance between every camera pair within a forest patch, and found that these were not significantly correlated with forest patch size (Fig A1.5).

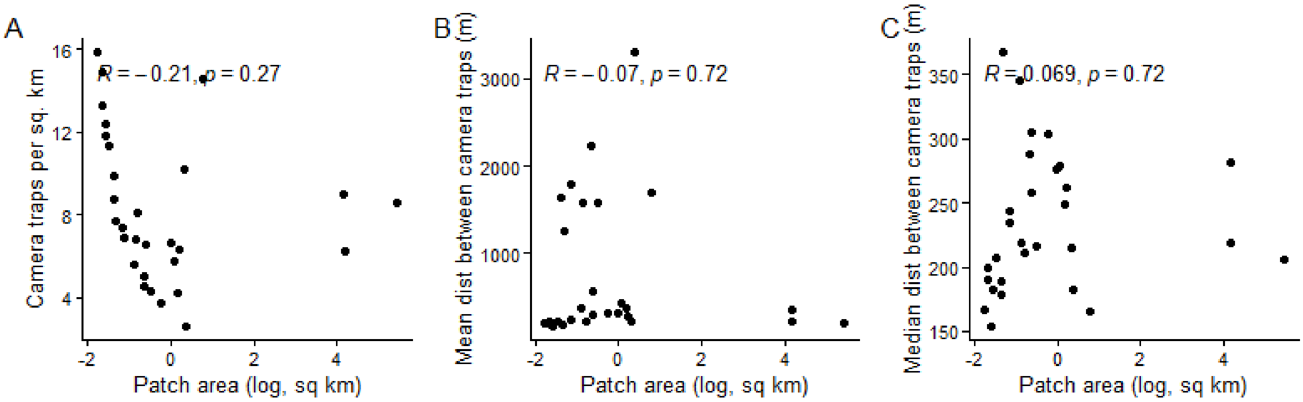

Figure A1.5. Correlation between forest patch size (log-transformed, sq. km) and camera trap density (A), mean distance between cameras in metres (B) and median distance between cameras in metres. R = Pearson's correlation coefficient.

A1.5. Evaluating Wildlife Insights AI algorithm

The in-built artificial intelligence (AI) image classification model in Wildlife Insights (www.wildlifeinsights.org; Ahumada et al., 2020) was used to detect and remove blank (i.e., false trigger) images. To evaluate the model's performance we calculated the precision and recall for identifying blank images and for detecting deer species. Precision is defined as the percentage of positive identifications by the model that were actually correct, while recall is defined as the percentage of actual positives that were correctly identified by the model.

We first evaluated the object detection model in Wildlife Insights which detects whether an animal is in the frame using a subset of 13,699 manually classified images spanning 28 forest patches from Aberdeenshire. We found that the AI model classified blank images with a precision of 99.01%. Given the high precision, we used the AI model to remove false trigger images from our dataset; for example, those caused by wind moving vegetation in front of the camera.

We then evaluated the precision and recall of the deer detection model in Wildlife Insights using a subset of 9754 images containing at least one animal (i.e., 'non-blank'). These images were manually classified, the number of animals counted, and the species identified to the highest level possible. We found that the model had a precision of 97.68% for images classified as 'Cervidae' and model recall of 89.43% for deer images. Additionally, we found only 3 occurrences of red deer (*Cervus elaphus*) limited to 2 out of the 30 forest patches in Aberdeenshire. 2100 images AI-classified as ‘Cervidae’ from these two sites were further manually screened to ensure no other images of red deer were present. Given the high precision and recall of deer detection by the AI model and the very low percentage of red deer images from Aberdeenshire, we categorised all images identified as ‘Cervidae’ by the AI model as roe deer. Images classified as ‘not-Cervidae’ were all reviewed and classified manually.

A1.6. Variable selection

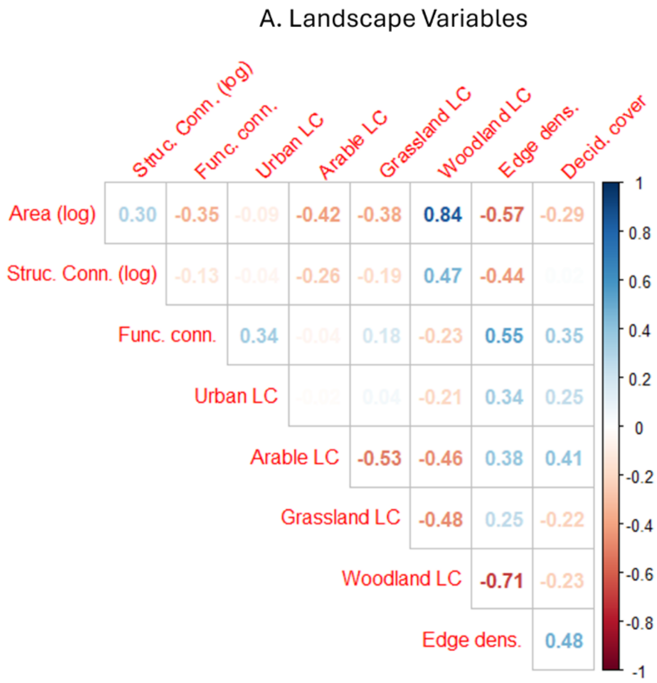

A. Landscape Variables

	Struc. Conn. (log)	Func. conn.	Urban LC	Arable LC	Grassland LC	Woodland LC	Edge dens.	Decid. cover
Area (log)	0.30	-0.35	-0.09	-0.42	-0.38	0.84	-0.57	-0.29
Struc. Conn. (log)		-0.13	-0.04	-0.26	-0.19	0.47	-0.44	0.02
Func. conn.			0.34	-0.04	0.18	-0.23	0.55	0.35
Urban LC				-0.02	0.04	-0.21	0.34	0.25
Arable LC					-0.53	-0.46	0.38	0.41
Grassland LC						-0.48	0.25	-0.22
Woodland LC							-0.71	-0.23
Edge dens.								0.48

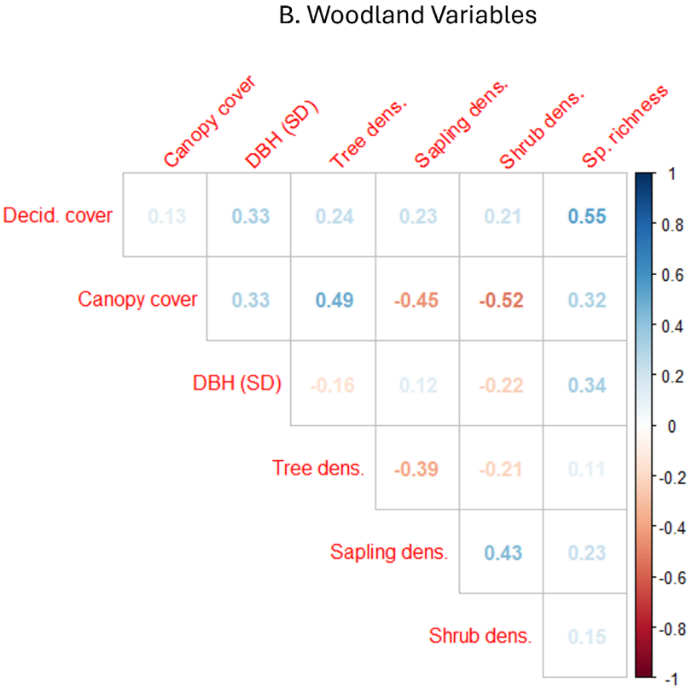

B. Woodland Variables

	Canopy cover	DBH (SD)	Tree dens.	Sapling dens.	Shrub dens.	Sp. richness
Decid. cover	0.13	0.33	0.24	0.23	0.21	0.55
Canopy cover		0.33	0.49	-0.45	-0.52	0.32
DBH (SD)			-0.16	0.12	-0.22	0.34
Tree dens.				-0.39	-0.21	0.11
Sapling dens.					0.43	0.23
Shrub dens.						0.15

Fig. A1.6: Correlation matrices for candidate landscape (A) and forest variables (B). Numbers inside the grids correspond to Pearson's correlation coefficients (r) for variable pairs. Variable pairs with r >0.7 were identified and the ones more relevant to the study questions included in the full models.

A1.7. Software availability

For all connectivity analyses we used R (v.4.4.2 and v. 4.4.1) (R Core Team, 2024), and RStudio (v.2024.12.0+467 and v.2024.09.1+394) (Posit team, 2024), and the following R packages. For analysis of animal movement data, we used amt (v.0.2.2.0) (Signer et al., 2019) and move (v.4.2.6) (Kranstauber et al., 2024). For general data manipulation we used glue (v.1.8.0) (Hester & Bryan, 2024), sjmisc (v.2.8.10) (Lüdecke, 2018a), tidyverse (v.2.0.0) (Wickham et al., 2019), and units (v.0.8.5) (Pebesma et al., 2016). For project and code management we used here (v.1.0.1) (Müller, 2020), tarchetypes (v.0.11.0) (Landau, 2021a), and targets (v.1.9.0) (Landau, 2021b). For visualisation we used the following as expansions from the tidyverse suite of packages: ggdist (v.3.3.2) (Kay, 2024a,b), ggplot2 (v.3.5.2) (Wickham, 2016), ggridges (v.0.5.6) (Wilke, 2024), ggtext (v.0.1.2) (Wilke & Wiernik, 2022), patchwork (v.1.3.0) (Pedersen, 2024), and scales (v.1.3.0) (Wickham et al., 2023). Other packages we used were boot (v.1.3.31) (Davison & Hinkley, 1997; Canty & Ripley, 2024), circular (v.0.5.1) (Agostinelli & Lund, 2024), doParallel (v.1.0.17) (Microsoft Corporation & Weston, 2022), foreach (v.1.5.2) (Microsoft & Weston, 2022), knitr (v.1.49) (Xie, 2014, 2015, 2024), and usethis (v.3.0.0) (Wickham et al., 2024). To manipulate and manage spatial data we used gdistance (v.1.6.4) (van Etten, 2017), mgc (v.2.0.2) (Bridgeford et al., 2020), raster (v.3.6.30 and v.3.6.31) (Hijmans, 2024a), sf (v.1.0.19) (Pebesma, 2018; Pebesma & Bivand, 2023), sp (v.2.1.4 and v.2.2.0) (Pebesma & Bivand, 2005; Bivand, et al., 2013), terra (v.1.7.83 and v.1.8.29) (Hijmans, 2024b), and tidyterra (v.0.6.1) (Hernangómez, 2023) and QGIS (v.3.40.2) (Quantum GIS Development Team, 2025). To run models and explore model outputs we used DHARMa (v.0.4.7) (Hartig, 2022), effects (v.4.2.2) (Fox, 2003; Fox & Hong, 2009; Fox & Weisberg, 2018, 2019), ggeffects (v.2.2.1) (Lüdecke, 2018b), glmmTMB (v.1.1.10) (Brooks et al., 2017), INLA (v.24.6.27) (Martins et al., 2013; Lindgren & Rue, 2015), lme4 (v.1.1.35.5) (Bates et al., 2015), and performance (v.0.12.4 and v.0.13.0) (Lüdecke et al., 2021).

Additionally, scripts used to generate functionality connectivity measures are available at: https://github.com/BenMMarshall/TICKSOLVE_DeerMovement; and archived at: https://doi.org/10.5281/zenodo.18701055 (Marshall., 2026).

For the graphical abstract visuals, we used Blender 4.5 LTS (Blender Online Community, 2025) and Affinity Publisher 2 (Serif, 2025).

A2. Results

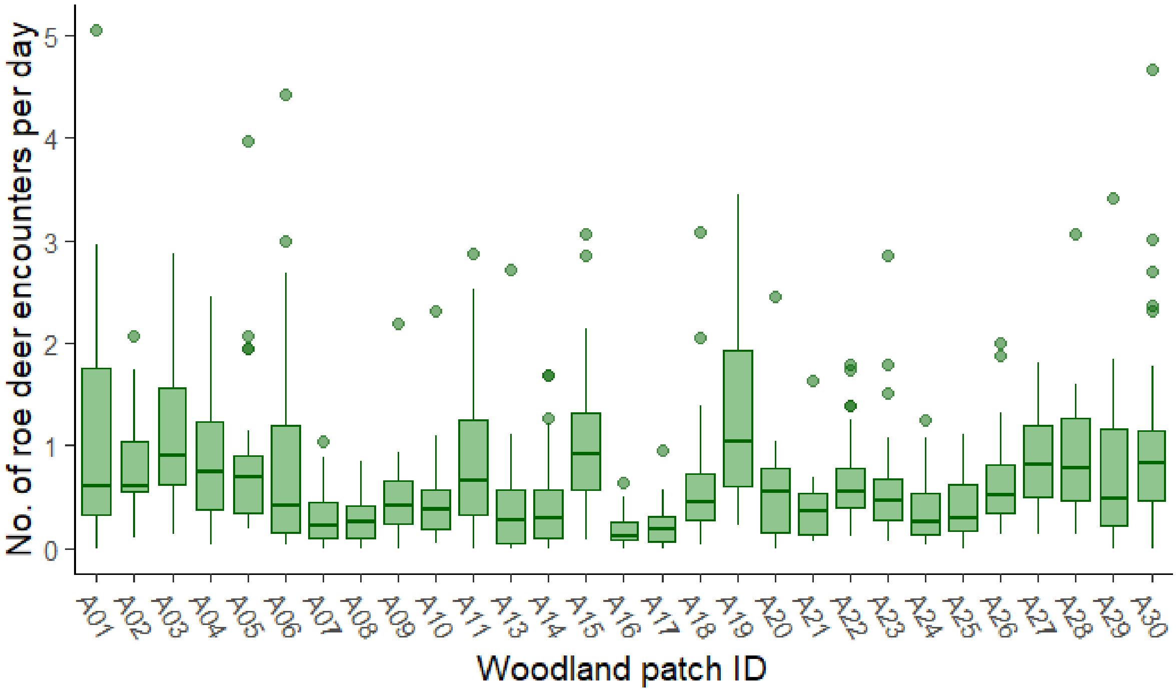

Fig. A2.1: Within and between site variation in roe deer encounter rates in forests.

A2.1. Drivers of roe deer forest use

Table A2.1 Summaries of final models obtained after model reduction. Model 1 included structural connectivity as an explanatory variable while Model 2 included functional connectivity, while all other explanatory variables were the same in the two full models. Estimates are exponentiated coefficients of the final negative binomial GLMMs. All *explanatory variables were mean centred and scaled. Estimates are rate ratios on the response scale.*

	Model 1			**Model 2**		
Predictors	*Estimate*	*95% CI*	*p*	*Estimate*	*95% CI*	*p*
Intercept	0.58	0.50 – 0.66	**<0.001**	0.58	0.50 – 0.66	**<0.001**
Area (log)	0.82	0.71 – 0.94	**0.006**			
Struc. connectivity (log)	1.18	1.03 – 1.36	**0.019**			
Func. connectivity				1.24	1.08 – 1.42	**0.002**
Dist. to wood. edge	0.91	0.83 – 0.99	**0.024**	0.90	0.83 – 0.98	**0.012**
DBH (SD)	1.25	1.08 – 1.44	**0.002**	1.28	1.11 – 1.48	**0.001**
Tree dens.	1.22	1.06 – 1.39	**0.004**	1.22	1.07 – 1.40	**0.003**
Human ER (Patch mean)	0.86	0.74 – 0.99	**0.032**	0.85	0.74 – 0.99	**0.031**
Random Effects						
σ^2*	1.09			1.09		
τ_{00}†	$0.14_{\text{month:year:patch ID}}$			$0.14_{\text{month:year:patch ID}}$		
	$0.08_{\text{year:patch ID}}$			$0.08_{\text{year:patch ID}}$		
	$0.04_{\text{patch ID}}$			$0.04_{\text{patch ID}}$		
N	6_{month}			6_{month}		
	2_{year}			2_{year}		
	$29_{\text{patch ID}}$			$29_{\text{patch ID}}$		
Observations	690			690		
Marginal R^2 / Conditional R^2‡	0.097 / 0.272			0.095 / 0.273		
AICc	5332.236			5330.521		

*σ^2: Residual variance equivalent for negative binomial mixed models (Nakagawa et al. 2017), †τ_{00}: Random intercept variance, ‡Marginal & conditional R^2 (Nakagawa et al. 2017)

Table A2.2: Summary of final reduced model fitted to test the effect of edge density on roe deer encounter rates. Full model included the same response and explanatory variables as Model 1 except forest area was replaced by edge density.

Predictors	*Estimate*	*95% CI*	*p*
Intercept	0.57	0.50 – 0.66	**<0.001**
Edge density (750m buffer)	1.21	1.04 – 1.42	**0.017**
Struc. connectivity (log)	1.21	1.04 – 1.40	**0.015**

Dist. to forest edge	0.90	0.82 – 0.97	**0.011**
DBH (SD)	1.30	1.12 – 1.51	**<0.001**
Tree dens.	1.19	1.03 – 1.36	**0.015**
Human ER (Patch mean)	0.84	0.73 – 0.98	**0.024**
Random Effects			
σ^2	1.09		
τ_{00} month_num:year:site_id	0.14		
τ_{00} year:site_id	0.08		
τ_{00} site_id	0.05		
N month_num	6		
N year	2		
N site_id	29		
Observations	690		
Marginal R^2 / Conditional R^2	0.090 / 0.270		
AICc	5333.701		

Table A2.3: Summary of final reduced model fitted to test the effect of forest cover in 750m buffer around patch on roe deer encounter rates. Full model included the same response and explanatory variables as Model 1 except forest area was replaced by forest cover in 750m buffer.

Predictors	*Estimate*	*95% CI*	*p*
Intercept	0.57	0.50 – 0.66	**<0.001**
Forest cover (750m buffer)	0.86	0.74 – 1.02	0.077
Dist. to forest edge	0.91	0.84 – 1.00	**0.044**
DBH (SD)	1.26	1.07 – 1.47	**0.005**
Tree dens.	1.16	1.00 – 1.34	**0.046**
Human ER (Patch mean)	0.86	0.73 – 1.00	0.052
Random Effects			

σ^2	1.09
$\tau_{00\ \mathrm{month\_num:year:site\_id}}$	0.13
$\tau_{00\ \mathrm{year:site\_id}}$	0.08
$\tau_{00\ \mathrm{site\_id}}$	0.07
$N_{\mathrm{month\_num}}$	6
N_{year}	2
$N_{\mathrm{site\_id}}$	29
Observations	690
Marginal R^2 / Conditional R^2	0.080 / 0.274
AICc	5335.987

A2.2. Drivers of roe deer functional connectivity

Table A2.4: Summary of the linear model with mean roe deer functional connectivity as the response variable and landscape metrics as the explanatory variables.

Predictors	*Estimates*	*95% CI*	*p*
(Intercept)	0.060	0.053 – 0.068	**<0.001**
Area (log)	-0.009	-0.018 – -0.000	**0.042**
Struc. conn	-0.003	-0.011 – 0.006	0.509
Decid. cover	0.009	0.000 – 0.018	**0.050**
Arable 750m	-0.009	-0.018 – 0.000	0.051
Urban 750m	0.005	-0.002 – 0.013	0.174
Observations	29		
R^2 / R^2 adj.	0.347 / 0.169		
AICc	-123.2815		

Table A2.5: Model reduction table for Model1 and 2 with the AICs of full, intermediate and final models. The variables dropped at each step of model reduction are included in the table alongside the AIC of the intermediate model once the corresponding variable was dropped. DeltaAICs were calculated for as the difference in AIC between the full or intermediate model, and the final model. Model reduction was carried out starting with the second-order coefficient of structural (Model 1) and functional connectivity (Model 2) respectively. The final *step refers to the final variable dropped to obtain the final reduced model and its AIC. See Table A2.1 for the final model summaries for Model 1 and 2.*

Step	Removed term	AIC	deltaAIC
A) <u>Model 1</u>			
Full model		5347.636	11.972
1	Struc. connectivity (log)[2]	5345.653	9.989
2	Sapling dens. (log)	5343.653	7.990
3	Woody debris	5341.654	5.990
4	Tree species richness	5339.657	3.993
5	Deciduous cover	5339.657	3.993
6	Shrub dens. (log)	5337.695	2.032
7	Arable land cover	5337.695	2.032
8	Canopy closure (%)	5335.786	0.123
9	Urban land cover (%) – *Final model*	5335.664	0
B) <u>Model 2</u>			
Full model		5345.941	15.744
1	Func. connectivity (log)[2]	5344.204	14.006
2	Urban land cover	5342.217	12.0194
3	Canopy closure (%)	5340.238	10.041
4	Tree species richness	5339.122	8.925
5	Deciduous cover	5337.127	6.930
6	Arable land cover	5335.263	5.066
7	Woody debris	5333.757	3.559
8	Shrub dens. (log)	5332.507	2.310
9	Sapling dens. (log)	5330.924	0.727
10	Area (log) – *Final model*	5330.197	0

Appendix References

Agostinelli C, Lund U. 2024. R package circular: Circular statistics (version 0.5-1).

Ahumada, J. A., Fegraus, E., Birch, T., Flores, N., Kays, R., O'Brien, T. G.,…Dancer, A. 2020. Wildlife Insights: A Platform to Maximize the Potential of Camera Trap and Other Passive Sensor Wildlife Data for the Planet. *Environmental Conservation*, *47*(1), 1-6. https://doi.org/10.1017/S0376892919000298

Bates D, Mächler M, Bolker B, Walker S. 2015. Fitting linear mixed-effects models using lme4. *Journal of Statistical Software* 67:1–48. https://doi.org/10.18637/jss.v067.i01.

Bender DJ, Tischendorf L, Fahrig L. 2003. Using patch isolation metrics to predict animal movement in binary landscapes. *Landscape Ecology*, *18*(1), 17–39. https://doi.org/10.1023/A:1022937226820

Blender Online Community. (2025). Blender—A 3D modelling and rendering package. Blender Foundation. http://www.blender.org

Bivand RS, Pebesma E, Gomez-Rubio V. 2013. Applied spatial data analysis with R, second edition. Springer, NY.

Bridgeford E, Shen C, Wang S. 2020. mgc: Multiscale Graph Correlation.

Brooks ME, Kristensen K, van Benthem KJ, Magnusson A, Berg, CW, Skaug AN,…Bolker BM. 2017. glmmTMB Balances Speed and Flexibility Among Packages for Zero-inflated Generalized Linear Mixed Modeling. *The R Journal*, *9*(2), 378-400. https://doi.org/10.32614/RJ-2017-066

Canty A, Ripley B. 2024. boot: Bootstrap R (S-Plus) Functions.

Microsoft Corporation, Weston S. 2022. doParallel: Foreach parallel adaptor for the “parallel” package.

Davison AC, Hinkley DV. 1997. Bootstrap Methods and Their Application. Cambridge University Press.

Forestry Commission. 2019. *National Forest Inventory Woodland Map 2019 (GB)* [Data set]. https://www.data.gov.uk/dataset/4f73f738-5c3f-4b40-8a8e-0ccae715de2f/national-forest-inventory-woodland-map-2019-gb.

Fox J, Hong J. 2009. Effect displays in R for multinomial and proportional-odds logit models: Extensions to the effects package. *Journal of Statistical Software* 32:1–24. https://doi.org/ 10.18637/jss.v032.i01.

Fox J, Weisberg S. 2018. Visualizing fit and lack of fit in complex regression models with predictor effect plots and partial residuals. *Journal of Statistical Software* 87:1–27. https://doi.org/10.18637/jss.v087.i09.

Fox J, Weisberg S. 2019. An r companion to applied regression. Thousand Oaks CA: Sage.

Fox J. 2003. Effect displays in R for generalised linear models. *Journal of Statistical Software* 8:1–27. https://doi.org/10.18637/jss.v008.i15.

Gill RMA, Morgan G. 2010. The effects of varying deer density on natural regeneration in woodlands in lowland Britain. *Forestry: An International Journal of Forest Research* 83(1): 53–63. https://doi.org/10.1093/forestry/cpp031

Hanski I. 1998. Metapopulation dynamics. *Nature 1998 396:6706*, *396*(6706), 41–49. https://doi.org/10.1038/23876

Hartig F. 2022. DHARMa: Residual Diagnostics for Hierarchical (Multi-Level / Mixed) Regression Models. In.

Hernangómez D. 2023. Using the tidyverse with terra objects: The tidyterra package. *Journal of Open Source Software* 8:5751. https://doi.org/10.21105/joss.05751.

Hester J, Bryan J. 2024. glue: Interpreted string literals.

Hijmans RJ. 2024a. raster: Geographic data analysis and modeling.

Hijmans RJ. 2024b. terra: Spatial data analysis.

Kay M. 2024a. ggdist: Visualizations of distributions and uncertainty in the grammar of graphics. *IEEE Transactions on Visualization and Computer Graphics* 30:414–424. https://doi.org/10.1109/TVCG.2023.3327195.

Kay M. 2024b. *ggdist: Visualizations of distributions and uncertainty*. https://doi.org/10.5281/zenodo.3879620.

Kranstauber B, Kays R, Lapoint SD, Wikelski M, Safi K. 2012. A dynamic Brownian bridge movement model to estimate utilization distributions for heterogeneous animal movement. *Journal of Animal Ecology* 81:738–746. https://doi.org/10.1111/j.1365-2656.2012.01955.x.

Kranstauber B, Smolla M, Scharf AK. 2024. move: Visualizing and analyzing animal track data.

Landau WM. 2021a. *tarchetypes: Archetypes for targets*.

Landau WM. 2021b. The targets r package: A dynamic make-like function-oriented pipeline toolkit for reproducibility and high-performance computing. *Journal of Open Source Software* 6:2959.

Lindgren F, Rue H. 2015. Bayesian spatial modelling with R-INLA. *Journal of Statistical Software* 63:1–25.

Lüdecke D, Ben-Shachar MS, Patil I, Waggoner P, Makowski D. 2021. performance: An R package for assessment, comparison and testing of statistical models. *Journal of Open Source Software* 6:3139. https://doi.org/10.21105/joss.03139.

Lüdecke D. 2018a. sjmisc: Data and variable transformation functions. *Journal of Open Source Software* 3:754. https://doi.org/10.21105/joss.00754.

Lüdecke D. 2018b. ggeffects: Tidy Data Frames of Marginal Effects from Regression Models. *Journal of Open Source Software* 3(26): 772.

Marshall BM, Gilbert L, Boyle J, Lhamine VV, Greener MS, Gill R, Millins C, Morrison TA. 2026a. Roe Deer show an affinity for woodland and reluctance to cross roads. EcoEvoRix https://doi.org/10.32942/X2JD47

Marshall B, Gilbert L, Boyle J, Lhamine V, Greener M, Gill R, Millins C, Morrison T. 2026b. Supporting Data for Roe Deer show an affinity for woodland and reluctance to cross roads (0.9.1) [Data set]. Zenodo. https://doi.org/10.5281/zenodo.18699746

Marshall BM. 2026. BenMMarshall/TICKSOLVE_DeerMovement: 0.9.1 Preprint (0.9.1). Zenodo. https://doi.org/10.5281/zenodo.18701056

Marston C, Rowland CS, O'Neil AW, Morton RD. 2022. Land Cover Map 2021 (25m rasterised land parcels, GB). In: NERC EDS Environmental Information Data Centre.

Martins TG, Simpson D, Lindgren F, Rue H. 2013. Bayesian computing with INLA: New features. *Computational Statistics and Data Analysis* 67:68–83.

Microsoft, Weston S. 2022. foreach: Provides foreach looping construct.

Morton D, Marston CG, O’Neil AW, Rowland CS. 2024. Land Cover Map 2023 (25m rasterised land parcels, GB). In: NERC EDS Environmental Information Data Centre.

Müller K. 2020. here: A simpler way to find your files.

Ordnance Survey. 2024. OS Open Roads v.2.4.

Panzacchi M, Van Moorter B, Strand O, Saerens M, Kivimäki I, St. Clair CC, Herfindal I, Boitani L. 2016. Predicting the *continuum* between corridors and barriers to animal movements using Step Selection Functions and Randomized Shortest Paths. *Journal of Animal Ecology* 85:32–42. https://doi.org/10.1111/1365-2656.12386.

Pebesma E, Bivand R. 2023. *Spatial Data Science: With applications in R*. Chapman and Hall/CRC. https://doi.org/10.1201/9780429459016.

Pebesma E, Mailund T, Hiebert J. 2016. Measurement units in R. *R Journal* 8:486–494. https://doi.org/10.32614/RJ-2016-061.

Pebesma E. 2018. Simple Features for R: Standardized Support for Spatial Vector Data. *The R Journal* 10:439–446. https://doi.org/10.32614/RJ-2018-009.

Pebesma EJ, Bivand R. 2005. Classes and methods for spatial data in R. *R News* 5:9–13.

Pedersen TL. 2024. patchwork: The composer of plots.

Posit team. 2024. RStudio: Integrated development environment for r. Boston, MA: Posit Software, PBC.

Prima M, Renaud J, Witté I, Suarez L, Rouveyrol P, Fernando M, Sacchi A, Cosentino F, Santini L, Maiorano L, Moreira F, Dertien J, Fernández N, Thuiller W. 2024. A comprehensive framework to assess multi-species landscape connectivity. *Methods in Ecology and Evolution* 15:2385–2399. https://doi.org/10.1111/2041-210X.14444.

Quantum GIS Development Team. (2025). Quantum GIS Geographic Information System [Computer software]. http://qgis.osgeo.org

R Core Team. 2024. R: A language and environment for statistical computing. Vienna, Austria: R Foundation for Statistical Computing.

Scholefield PA, Morton RD, Rowland CS, Henrys PA, Howard DC, Norton LR. 2016. Woody linear features framework, Great Britain v.1.0. https://doi.org/10.5285/D7DA6CB9-104B-4DBC-B709-C1F7BA94FB16.

Serif. (2025). Affinity Publisher 2 (Version 2.6.5) [Windows]. Serif Europe Ltd.

Signer J, Fieberg J, Avgar T. 2019. Animal movement tools (amt): R package for managing tracking data and conducting habitat selection analyses. *Ecology and Evolution* 9:880–890.

van Etten J. 2017. R package gdistance: Distances and routes on geographical grids. *Journal of Statistical Software* 76:1–21. https://doi.org/10.18637/jss.v076.i13.

Wickham H, Averick M, Bryan J, Chang W, McGowan LD, François R, Grolemund G, Hayes A, Henry L, Hester J, Kuhn M, Pedersen TL, Miller E, Bache SM, Müller K, Ooms J, Robinson D, Seidel DP, Spinu V, Takahashi K, Vaughan D, Wilke C, Woo K, Yutani H. 2019. Welcome to the tidyverse. *Journal of Open Source Software* 4:1686. https://doi.org/10.21105/joss.01686.

Wickham H, Bryan J, Barrett M, Teucher A. 2024. usethis: Automate package and project setup.

Wickham H, Pedersen TL, Seidel D. 2023. scales: Scale functions for visualization.

Wickham H. 2016. ggplot2: Elegant Graphics for Data Analysis. Springer-Verlag New York.

Wilke CO, Wiernik BM. 2022. ggtext: Improved text rendering support for “ggplot2”.

Wilke CO. 2024. ggridges: Ridgeline plots in “ggplot2”.

Xie Y. 2014. knitr: A Comprehensive Tool for Reproducible Research in R. *Implementing Reproducible Computational Research*. Chapman and Hall/CRC.

Xie Y. 2015. Dynamic Documents with R and knitr. Chapman & Hall/CRC.

Xie Y. 2024. knitr: A General-Purpose Package for Dynamic Report Generation in R.